PERGAMON

Organic Geochemistry 30 (1998) 161–188

Organic Geochemistry

Palaeoceanographic controls on geochemical characteristics of organic-rich Exshaw mudrocks: role of enhanced primary production

Mark L. Caplan *, R. Marc Bustin

Department of Earth and Ocean Sciences, The University of British Columbia, 6339 Store Road, Vancouver, BC, Canada V6T 1Z4

Received 27 August 1997; accepted 29 September 1998
(returned to author for revision 5 February 1998)

Abstract

Organic-rich source rocks have generally been attributed to enhanced preservation of organic matter under anoxic bottom waters. Here, geochemical analysis of kerogen and whole rock samples of organic-rich (lithofacies B_1) and organic-lean (lithofacies B_2) laminated mudrocks of the Devonian–Carboniferous Exshaw Formation, Alberta, highlight the importance of primary production in governing the quantity and quality of organic matter. Lower Si/Al, K/Al, Ti/Al and quartz/clay ratios in lithofacies B_2, similar maceral types and the laminated fabric of the two lithofacies indicate that the quality and quantity of organic matter are not related to grain size, redox or organic matter source changes. High Total Organic Carbon (TOC) and Hydrogen Index (HI), low Oxidation Index (Ox.I. ratio of oxygen functional groups to aliphatic groups derived by FTIR), lighter $\delta^{15}N_{tot}$ and heavier $\delta^{13}C_{org}$ isotopes indicate that kerogen of lithofacies B_1 accumulated during periods of high organic-carbon production and delivery of relatively fresh, labile, well-preserved organic matter to the sea floor. In contrast, low TOC, HI, high Ox.I., heavier $\delta^{15}N_{tot}$ and lighter $\delta^{13}C_{org}$ isotopes indicate low primary productivity and delivery, high recycling and poor preservation of organic matter during accumulation of lithofacies B_2.

Keywords: Devonian–Carboniferous; Black shales; palaeoproductivity; Exshaw Formation; palaeoceanography; anoxia; primary productivity

1. Introduction

The quality and quantity of organic carbon preserved in modern and ancient sediments is the result of a complex interaction of oceanographic and sedimentological factors, including primary productivity in the water column, allochthonous supply of organic matter, particle flux to the sea floor, redox-sensitive oxidation processes, sediment accumulation rates and sediment grain size (e.g. Demaison and Moore, 1980; Calvert, 1987; Tyson, 1987; Hollander et al., 1990; Pedersen and Calvert, 1990; Wignall, 1994; Tyson, 1995). The formation of organic-rich sedimentary facies is thought to be controlled mainly by benthic water column anoxia or supply of organic matter to the sea floor (e.g. Demaison and Moore, 1980; Pedersen and Calvert, 1990). This study aims at utilizing multidisciplinary information in order to address the question of identifying palaeoceanographic factors affecting or-

* Corresponding author. Present address. TOTAL, Scientific and Technical Centre, Route de Versailles, 78470, Saint-Rémy-lès-Chevreuse, France. E-mail: mark.caplan@total.com

0146-6380/99/$ - see front matter
PII: S0146-6380(98)00202-2

ganic matter preservation in the rock record, following the protocol of Huc et al. (1992) and Tribovillard et al. (1994).

Many studies have implied that benthic anoxia is a prerequisite for the preservation of organic matter and development of organic-rich mudrocks (e.g. Schlanger and Jenkyns, 1976; Demaison and Moore, 1980). Yet some laminated mudrocks reflecting deposition beneath anoxic bottom waters display variations in TOC (total organic carbon, reported as a weight per cent) and HI (hydrogen index; mg hydrocarbon per g TOC) that cannot be explained by source variations, clastic input or diagenetic changes in the sediment (e.g. Calvert et al., 1992a; Bertrand and Lallier-Verges,

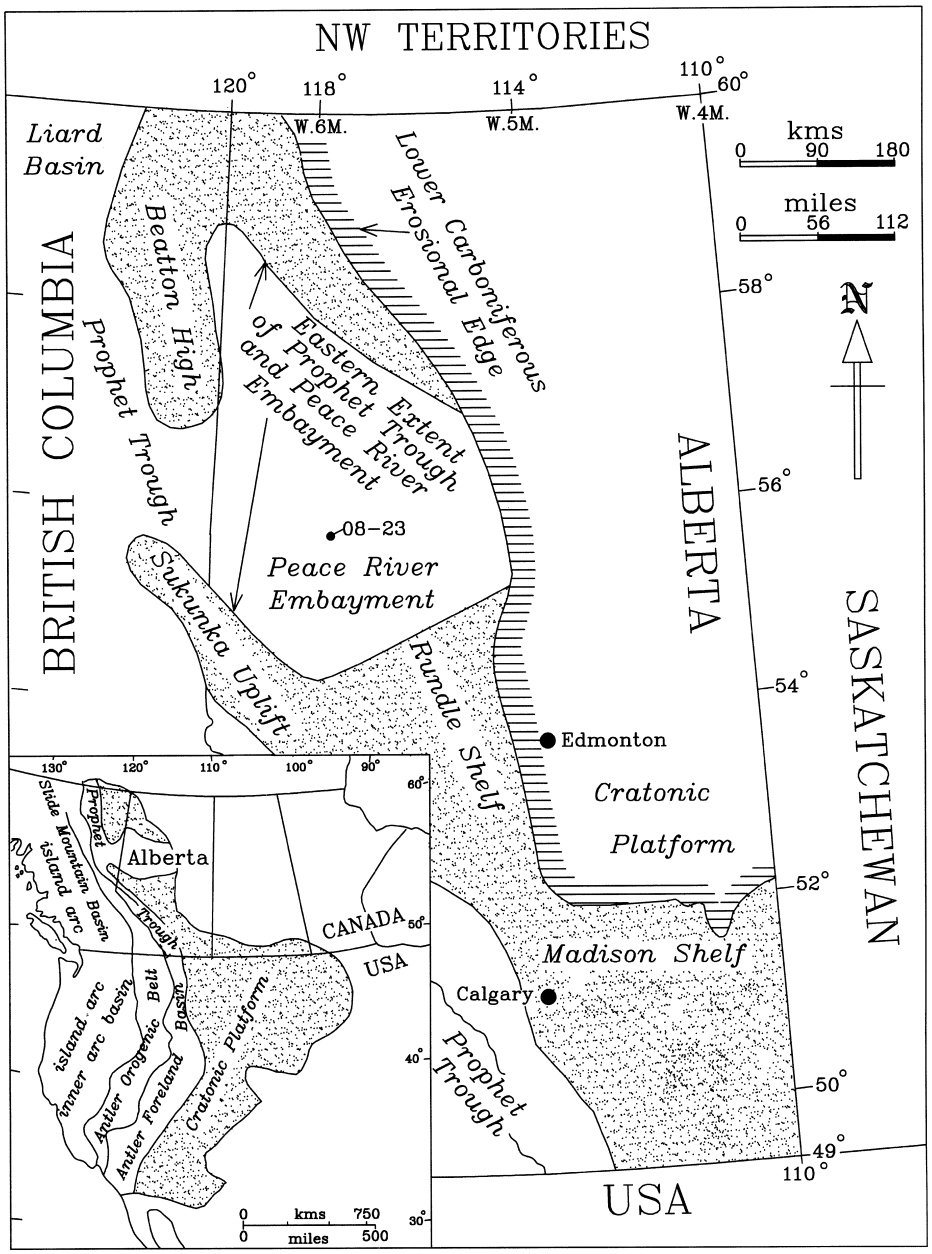

Fig. 1. Location map of study area and well 8-23-080-24W5; the insert shows regional palaeotectonic map of western North America during Devonian–Carboniferous times (after Richards, 1989). The Alberta cratonic platform (stippled region of main map) is divided into the Madison Shelf and Rundle Shelf.

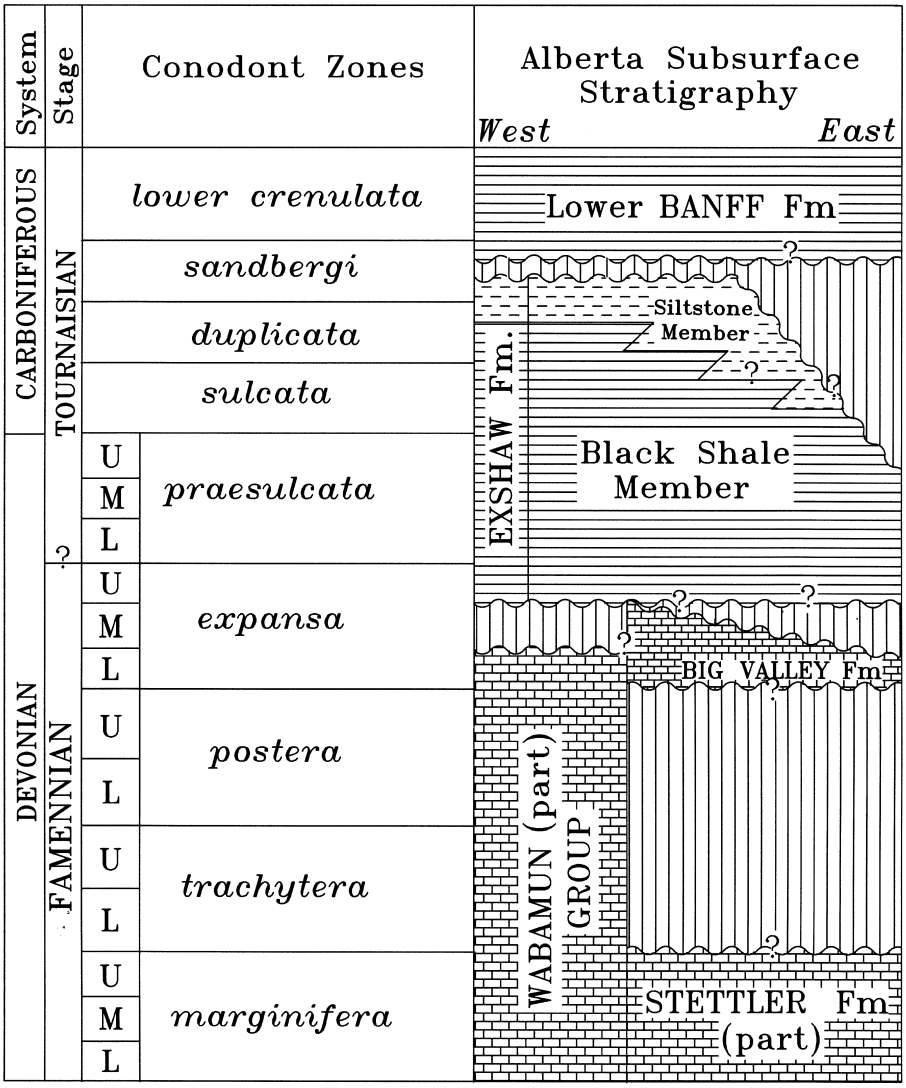

Fig. 2. Devonian–Carboniferous subsurface stratigraphy of Alberta (Macqueen and Sandberg, 1970; Richards and Higgins, 1988; Richards, 1989; Meijer Drees and Johnston, 1993).

1993; Bertrand et al., 1993; Tribovillard et al., 1994). The importance of anoxic bottom waters in governing organic-richness of sediments is now being questioned as recent findings show that sulphate reduction and oxic respiration oxidize equal amounts of organic matter in nearshore marine sediments (Jørgensen, 1982). Calvert (1987) documented that lipid-rich organic matter accumulates in modern sediments deposited on the continental shelf directly underlying regions of high primary productivity. The high supply of labile metabolizable organic matter to the sediments results in an enrichment of hydrogen-rich organic matter, and the subsequent consumption of dissolved oxygen from the bottom waters (Pedersen and Calvert, 1990). In this study, differing degrees of organic matter richness from two laminated Devonian mudrocks are attributed to fluctuations in primary productivity and the relative amount of labile organic carbon supply to the sea floor.

The laterally extensive Devonian–Carboniferous Exshaw Formation is an important petroleum source rock in the Western Canada Sedimentary Basin (Allan and Creaney, 1991). Although geochemical and sedimentological studies of this and similar source rocks have been undertaken, depositional conditions promoting such widespread shales and their organic-richness are poorly understood. In this study, organic-lean carbonate lithofacies of the Upper Devonian Big Valley

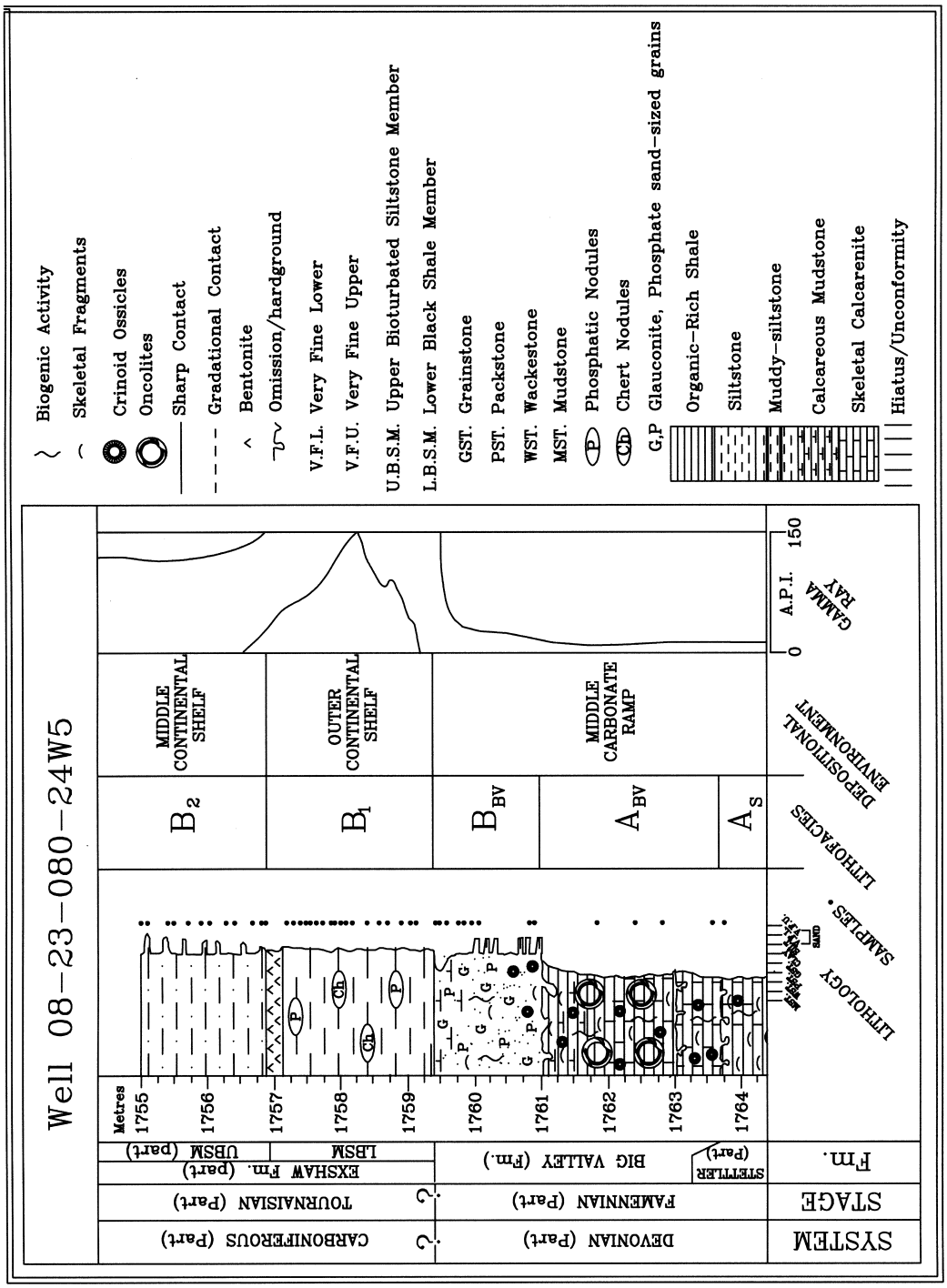

Fig. 3. Graphic log, gamma-ray response and sample locations derived from the Big Valley and Exshaw Formations from well 08-23-080-24W5, core interval 1755.00–1764.50 m.

Table 1
Geochemical characteristics of lithofacies B_1 and B_2 of the Exshaw Formation, B_{BV} and A_{BV} of the Big Valley Formation and A_S of the Settler Formation. Ox.I. denotes Oxidation Index (ratio of oxygenated functional groups to aliphatics from FTIR analysis). Average values for all geochemical parameters are included. Sample depths in driller depth.[a]

Sample #	Depth (m)	Lithofacies	Lithology	Kerogen Type	$\delta^{13}C$	$\delta^{15}N$	Ox.I.	T_{max}	S1	S2	S3	PI	S2/S3
1	1755.00	B2	clayshale	III	−28.27	1.96	–	430	0.48	5.16	0.48	0.09	10.75
2	1755.10	B2	clayshale	II	−28.63	1.78	1.99	430	1.33	12.38	0.31	0.10	39.93
5	1755.40	B2	clayshale	II	−28.58	1.34	1.14	430	1.59	12.28	0.31	0.11	39.61
6	1755.50	B2	clayshale	II	–	–	0.96	430	1.08	9.65	0.34	0.10	28.38
8	1755.70	B2	clayshale	II	−28.48	1.71	1.85	430	1.07	11.18	0.32	0.09	34.93
10	1755.90	B2	clayshale	II	–	–	0.87	432	1.58	12.72	0.42	0.11	30.28
11	1756.04	B2	clayshale	II	−28.75	1.58	–	430	1.15	11.63	0.45	0.09	25.84
14	1756.31	B2	clayshale	II	−28.64	1.75	1.39	429	1.14	10.28	0.51	0.10	20.15
15	1756.41	B2	clayshale	II	–	–	0.68	430	1.43	11.25	0.57	0.11	19.73
18	1756.70	B2	clayshale	III	−28.23	2.97	3.50	431	1.08	11.78	0.79	0.08	14.91
19	1756.80	B2	clayshale	III	−28.52	1.66	1.33	430	0.92	10.43	0.98	0.08	10.64
20	1756.84	B2	clayshale	III	−28.43	1.15	1.31	430	0.83	10.46	0.86	0.07	12.16
21	1757.19	B1	mudshale	III	−28.33	−0.37	0.27	428	5.98	67.23	1.65	0.08	40.74
22	1757.29	B1	mudshale	III	−28.51	−0.02	–	429	1.14	10.28	0.51	0.10	20.15
23	1757.39	B1	mudshale	III	–	–	0.32	427	1.96	20.86	1.22	0.09	17.09
24	1757.49	B1	mudshale	II	−28.26	0.01	0.57	424	5.96	76.26	1.70	0.07	44.85
26	1757.53	B1	mudshale	I	–	–	0.25	431	5.50	53.91	0.97	0.09	55.57
27	1757.63	B1	mudshale	I	−27.88	1.04	0.27	429	6.40	62.94	1.22	0.09	51.59
28	1757.73	B1	mudshale	I	–	–	0.13	425	5.95	35.64	0.72	0.14	49.50
29	1757.85	B1	mudshale	I	–	–	0.37	426	6.08	72.75	0.94	0.08	77.39
30	1757.90	B1	mudshale	II	−28.45	−0.02	–	428	5.98	67.23	1.65	0.08	40.74
31	1758.00	B1	mudshale	I	–	–	0.53	424	5.98	96.92	1.41	0.06	68.73
32	1758.10	B1	mudshale	II	–	–	0.45	421	3.21	34.72	1.00	0.08	34.72
33	1758.20	B1	mudshale	I	−28.37	0.56	0.44	428	5.91	96.65	1.39	0.06	69.53
35	1758.40	B1	mudshale	I	−28.44	−0.27	0.35	430	4.98	75.09	0.99	0.06	75.84
37	1758.62	B1	mudshale	I	−28.20	−0.18	0.46	431	7.06	148.20	1.27	0.05	116.69
38	1758.72	B1	mudshale	I	−28.17	−0.17	0.36	430	6.90	128.56	0.99	0.05	129.85
40	1758.92	B1	mudshale	II	−28.13	−0.09	–	429	6.4	62.94	1.22	0.09	51.59
41	1759.04	B1	mudshale	II	−28.12	0.29	0.50	427	4.04	72.36	1.60	0.05	45.22
42	1759.14	B1	mudshale	II	−27.8	0.46	–	426	3.36	48.74	1.31	0.06	37.2
43	1759.34	BBV	grainstone	III	−26.92	1.25	1.25	426	0.11	0.36	0.87	0.24	0.41
44	1759.44	BBV	grainstone	IV	−27.47	2.03	–	418	0.33	0.33	2.10	0.50	0.15
45	1759.66	BBV	grainstone	IV	−27.40	1.21	0.62	419	0.09	0.10	1.79	0.50	0.05
46	1759.76	BBV	grainstone	III	−27.37	1.31	0.55	421	0.24	0.73	1.41	0.25	0.51
47	1759.86	BBV	grainstone	III	−27.18	2.70	1.44	421	0.19	0.34	0.88	0.37	0.38
48	1759.96	BBV	grainstone	IV	–	–	1.57	413	0.14	0.14	1.08	0.50	0.12
49	1760.06	BBV	grainstone	IV	−27.49	1.14	–	419	0.10	0.10	0.93	0.50	0.10
50	1760.84	BBV	grainstone	IV	–	–	–	–	0.10	0.00	0.55	1.00	0.00
51	1760.91	ABV	oncolite pckst.	IV	−26.76	2.39	–	–	0.02	0.14	0.86	0.12	0.16
52	1761.85	ABV	oncolite pckst.	–	−27.70	2.94	–	–	–	–	–	–	–
53	1762.40	ABV	oncolite pckst.	–	−26.07	2.85	–	–	–	–	–	–	–
54	1762.82	ABV	oncolite pckst.	–	−26.75	3.70	–	–	–	–	–	–	–
55	1763.60	ABV	oncolite pckst.	–	−27.57	3.18	–	–	–	–	–	–	–
56	1763.75	AS	Stettler	–	−28.49	2.14	–	–	–	–	–	–	–
			average B2	II/III	−28.50	1.77	1.50	430	1.14	10.77	0.53	0.09	23.94
			average B1	I/II	−28.22	0.10	0.38	427	5.16	68.40	1.21	0.08	57.06
			average ABV	IV	−27.31	1.61	1.09	20	0.16	0.26	1.20	0.48	0.22
			average BBV	IV	−26.97	3.01	–	–	0.02	0.14	0.86	0.12	0.16

[a] Parameter dimensions are T_{max} (°C), S1 (mg HC/g rock), S2 (mg HC/g rock), S3 (mg CO_2/g rock) and PI (S1/[S2/S3]).

Formation, and organic-lean and organic-rich, laminated mudrocks from the overlying Devonian–Carboniferous Exshaw Formation are investigated geochemically to determine geological and palaeoceanographic processes responsible for variation in organic matter preservation.

Table 2
Geochemical characteristics of lithofacies B_1 and B_2 of the Exshaw Formation, B_{BV} and A_{BV} of the Big Valley Formation and A_S of the Stettler Formation. HI* and OI* denote hydrogen and oxygen indices derived from kerogen concentrates (continued).[a]

Sample #	PC	TOC	HI	OI	HI*	OI*	Mo/Al	Quartz/Clay	Fe (wt%)	Mn (wt%)	Ti (wt%)	Ca (wt%)	K (wt%)	Si (wt%)	Al (wt%)
1	0.47	1.96	263	24	–	–	1.7	3.2	4.3	0.0	0.7	0.4	3.66	0.4	11.8
2	1.14	3.29	376	9	305	7	3.5	3.0	4.6	0.0	0.7	0.4	3.45	8.2	12.6
5	1.15	3.47	353	8	460	8	3.3	2.5	4.4	0.0	0.7	0.4	3.65	8.7	13.3
6	0.89	3.20	301	10	351	5	–	–	–	–	–	–	–	–	–
8	1.02	3.39	329	9	341	5	3.4	3.7	4.0	0.0	0.7	0.5	3.65	8.9	13.3
10	1.19	3.37	377	12	359	6	–	–	–	–	–	–	–	–	–
11	1.06	3.19	364	14	–	–	3.0	3.2	3.9	0.0	0.7	0.4	3.76	0.7	13.8
14	0.95	2.92	352	17	308	6	3.2	–	4.3	0.0	0.7	0.4	3.65	9.5	13.7
15	1.05	1.89	595	30	311	6	–	–	–	–	–	–	–	–	–
18	1.07	3.10	380	25	394	9	–	2.6	–	–	–	–	–	–	–
19	0.94	2.98	350	32	366	4	3.1	3.7	3.0	0.0	0.7	0.4	3.46	0.7	11.7
20	0.94	2.50	418	34	279	7	2.5	3.3	3.0	0.0	0.7	0.5	3.4	65.1	12.5
21	6.10	10.56	636	15	661	5	17.6	6.0	2.1	0.0	0.3	0.5	1.8	69.5	5.7
22	0.95	2.92	352	17	–	–	18.5	10.3	2.0	0.0	0.3	1.9	1.5	66.4	4.7
23	1.90	4.37	477	27	511	6	–	–	–	–	–	–	–	–	–
24	6.85	11.23	679	15	509	3	19.1	4.3	4.2	0.0	0.4	3.8	2.4	54.1	7.2
26	4.95	5.93	909	16	528	3	–	–	–	–	–	–	–	–	–
27	5.77	9.69	649	12	496	3	7.4	–	2.2	0.0	0.4	5.0	1.9	56.0	5.4
28	3.46	6.09	585	11	623	2	–	–	–	–	–	–	–	–	–
29	6.56	10.16	716	9	600	3	–	–	–	–	–	–	–	–	–
30	6.10	10.56	636	15	–	–	15.4	3.3	2.9	0.0	0.4	7.7	2.7	48.7	7.6
31	8.57	15.89	609	8	502	5	–	–	–	–	–	–	–	–	–
32	3.16	5.97	581	16	492	4	–	–	–	–	–	–	–	–	–
33	8.54	12.85	752	10	637	3	–	–	–	–	–	–	–	–	–
35	6.67	10.93	687	9	683	4	8.8	6.0	2.0	0.0	0.4	9.8	2.5	51.1	6.8
37	12.93	17.56	843	7	704	5	–	–	–	–	–	–	–	–	–
38	11.28	16.43	782	6	689	4	5.8	4.8	2.9	0.0	0.4	3.8	2.9	50.1	7.0
40	5.77	9.69	649	12	–	–	–	–	–	–	–	–	–	–	–
41	6.36	10.69	676	14	–	–	6.6	3.3	6.4	0.0	0.6	5.6	3.7	46.3	10.3
42	4.34	7.53	647	17	–	–	2.1	4.0	2.9	0.0	0.6	10.4	4.1	45.1	8.6
43	0.03	0.17	211	511	301	10	1.9	4.0	0.9	0.1	0.0	47.2	0.5	11.7	1.2
44	0.05	0.42	78	500	–	–	1.2	3.0	1.4	0.1	0.1	42.5	0.7	16.0	1.9
45	0.01	0.14	71	1278	316	15	1.7	5.0	1.2	0.1	0.0	44.6	0.6	13.7	1.4
46	0.08	0.51	143	276	396	12	0.7	4.0	2.8	0.1	0.2	35.6	1.7	19.8	4.4
47	0.04	0.15	226	586	463	28	0.8	6.0	1.3	0.1	0.0	46.9	0.4	11.0	1.0
48	0.02	0.16	87	675	274	24	–	–	–	–	–	–	–	–	–
49	0.01	0.14	71	664	–	–	–	–	–	–	–	–	–	–	–
50	0.00	0.03	0	1833	–	–	–	–	–	–	–	–	–	–	–
51	0.01	0.03	466	2866	–	–	–	–	–	–	–	–	–	–	–
52	–	–	–	–	–	–	–	–	–	–	–	–	–	–	–
53	–	–	–	–	–	–	–	–	–	–	–	–	–	–	–
54	–	–	–	–	–	–	–	–	–	–	–	–	–	–	–
55	–	–	–	–	–	–	–	–	–	–	–	–	–	–	–
56	–	–	–	–	–	–	–	–	–	–	–	–	–	–	–
	0.99	2.94	372	19	347	6	2.9	3.1	3.9	0.0	0.7	0.4	3.5	60.3	12.8
	6.13	9.95	659	13	587	4	11.2	5.2	3.1	0.0	0.4	5.4	2.6	54.2	7.0
	0.03	0.22	111	790	350	18	1.3	4.4	1.5	0.1	0.1	43.3	0.8	14.4	2.0
	0.01	0.03	466	2866	–	–	–	–	–	–	–	–	–	–	–

[a] Refer to Table 1 for sample depths. Parameter dimensions are PC (0.83 [S1 + S2]), TOC (wt.% Corg), HI (mg HC/g Corg) and OI (mg CO_2/g Corg).

Table 3
Geochemical characteristics of lithofacies B_1 and B_2 of the Exshaw Formation, B_{BV} and A_{BV} of the Big Valley Formation and A_S of the Stettler Formation (continued).[a]

Sample #	Mg (wt%)	P (wt%)	Na (wt%)	C (wt%)	N (wt%)	S (wt%)	Nb (ppm)	Zr (ppm)	Y (ppm)	Sr (ppm)	Rb (ppm)	Pb (ppm)	Zn (ppm)	Cu (ppm)
1	1.1	0.1	0.4	2.1	0.1	2.7	5	114	28	108	160	21	212	27
2	1.5	0.1	0.0	3.2	0.2	2.9	5	120	30	100	145	13	357	31
5	1.4	0.1	0.5	3.2	0.1	2.6	5	112	29	102	154	11	332	28
6	–	–	–	–	–	–	–	–	–	–	–	–	–	–
8	1.3	0.1	0.7	3.5	0.2	2.3	8	111	28	103	157	16	318	28
10	–	–	–	–	–	–	–	–	–	–	–	–	–	–
11	1.5	0.1	0.5	3.4	0.2	3.3	5	117	30	98	158	13	333	32
14	1.4	0.1	0.5	3.2	0.2	2.3	7	121	30	108	154	16	341	31
15	–	–	–	–	–	–	–	–	–	–	–	–	–	–
18	–	–	–	3.4	0.2	1.8	9	122	31	114	146	19	411	29
19	1.3	0.1	0.3	3.2	0.1	1.3	9	121	30	109	141	13	633	25
20	1.6	0.2	0.9	2.9	0.1	1.1	10	119	33	117	131	8	528	22
21	0.8	0.2	0.4	11.4	0.4	1.6	6	59	25	52	56	6	63	35
22	0.7	0.3	0.0	9.1	0.3	1.4	3	42	28	58	38	2	195	32
23	–	–	–	–	–	–	–	–	–	–	–	–	–	–
24	1.1	0.3	0.3	14.0	0.4	2.9	6	76	34	72	74	23	27	53
26	–	–	–	–	–	–	–	–	–	–	–	–	–	–
27	1.7	0.1	0.5	12.0	0.3	1.8	6	60	21	82	63	16	18	38
28	–	–	–	–	–	–	–	–	–	–	–	–	–	–
29	–	–	–	–	–	–	–	–	–	–	–	–	–	–
30	1.2	0.5	0.4	13.6	0.4	2.3	6	89	40	113	76	19	26	48
31	–	–	–	–	–	–	–	–	–	–	–	–	–	–
32	–	–	–	–	–	–	–	–	–	–	–	–	–	–
33	–	–	–	–	–	–	–	–	–	–	–	–	–	–
35	1.3	0.4	0.0	12.7	0.3	1.8	5	91	39	138	66	16	22	49
37	–	–	–	–	–	–	–	–	–	–	–	–	–	–
38	0.6	0.3	0.3	20.2	0.7	5.3	4	68	30	79	69	20	670	87
40	–	–	–	–	–	–	–	–	–	–	–	–	–	–
41	1.4	0.4	0.2	12.5	0.4	4.3	4	119	32	110	104	44	100	70
42	1.0	2.5	0.2	9.4	0.3	1.1	13	196	107	306	70	21	27	48
43	0.6	0.5	0.0	10.7	0.0	0.0	0	22	18	349	13	12	11	5
44	0.7	0.5	0.0	9.9	0.0	0.0	2	29	16	292	16	14	13	1
45	0.8	0.5	0.1	10.2	0.0	0.0	2	21	13	285	23	10	12	3
46	1.4	0.6	0.0	8.4	0.0	0.1	4	66	26	280	45	17	13	5
47	0.7	0.5	0.0	10.5	0.0	0.1	1	18	15	306	17	15	10	3
48	–	–	–	–	–	–	–	–	–	–	–	–	–	–
49	–	–	–	–	–	–	–	–	–	–	–	–	–	–
50	–	–	–	–	–	–	–	–	–	–	–	–	–	–
51	–	–	–	–	–	–	–	–	–	–	–	–	–	–
52	–	–	–	–	–	–	–	–	–	–	–	–	–	–
53	–	–	–	–	–	–	–	–	–	–	–	–	–	–
54	–	–	–	–	–	–	–	–	–	–	–	–	–	–
55	–	–	–	–	–	–	–	–	–	–	–	–	–	–
56	–	–	–	–	–	–	–	–	–	–	–	–	–	–
	1.4	0.1	0.5	3.1	0.1	2.2	7	117	30	106	150	14	385	28
	1.1	0.6	0.3	12.8	0.4	2.5	6	89	39	112	68	19	128	51
	0.8	0.5	0.0	9.9	0.0	0.1	2	31	17	303	23	14	12	3
	–	–	–	–	–	–	–	–	–	–	–	–	–	–

[a] Refer to Table 1 for sample depth.

Table 4
Geochemical characteristics of lithofacies B_1 and B_2 of the Exshaw Formation, B_{BV} and A_{BV} of the Big Valley Formation and A_S of the Stettler Formation (continued).[a]

Sample #	Ni (ppm)	Co (ppm)	Mn (ppm)	V (ppm)	Cr (ppm)	Ba (ppm)	Na (ppm)	Mo (ppm)
1	128	16	51	608	112	398	1	20
2	215	19	71	1023	114	381	1	44
5	170	17	64	1013	113	401	1	44
6	–	–	–	–	–	–	–	–
8	159	16	59	1059	118	422	1	45
10	–	–	–	–	–	–	–	–
11	159	15	54	999	110	397	1	41
14	175	16	57	1026	117	420	1	43
15	–	–	–	–	–	–	–	–
18	275	16	70	1007	113	395	1	42
19	269	15	57	923	102	370	1	36
20	247	17	47	904	107	373	1	32
21	267	9	9	805	58	83	0	101
22	180	9	28	589	40	65	0	87
23	–	–	–	–	–	–	–	–
24	252	15	102	984	74	125	1	138
26	–	–	–	–	–	–	–	–
27	121	9	157	338	61	89	0	40
28	–	–	–	–	–	–	–	–
29	–	–	–	–	–	–	–	–
30	196	11	188	931	70	133	1	116
31	–	–	–	–	–	–	–	–
32	–	–	–	–	–	–	–	–
33	–	–	–	–	–	–	–	–
35	142	8	149	496	72	148	0	60
37	–	–	–	–	–	–	–	–
38	205	11	64	365	80	133	0	40
40	–	–	–	–	–	–	–	–
41	144	11	112	388	94	193	1	68
42	108	10	96	241	70	189	1	18
43	5	3	714	0	5	0	0	2
44	2	7	1095	1	11	5	0	2
45	3	5	1437	2	3	5	0	2
46	11	9	1062	13	19	10	0	3
47	0	4	1349	2	4	5	0	1
48	–	–	–	–	–	–	–	–
49	–	–	–	–	–	–	–	–
50	–	–	–	–	–	–	–	–
51	–	–	–	–	–	–	–	–
52	–	–	–	–	–	–	–	–
53	–	–	–	–	–	–	–	–
54	–	–	–	–	–	–	–	–
55	–	–	–	–	–	–	–	–
56	–	–	–	–	–	–	–	–
	200	16	59	951	112	395	1	38
	179	10	101	571	69	129	0	74
	4	5	1132	4	8	5	0	2
	–	–	–	–	–	–	–	–

[a] Refer to Table 1 for sample depth.

2. Methods

Powdered samples from a 6 m cored interval (well Canadian Superior Tangent 8–23, location 08-23-080-24W5) in northern Alberta (Figs. 1–3; Tables 1–4), were analyzed by Rock-Eval® to determine total organic carbon (TOC), level of thermal maturity and organic carbon type using standard pyrolysis procedures

(Espitalié et al., 1977; Peters, 1986). This well was chosen for its good core recovery and thermal immaturity of organic matter (T_{max} ranging from 413 to 432°C and strong yellow-green fluorescence of liptinite macerals). X-ray fluorescence spectrometry was employed following the procedure of Calvert (1990) to determine the concentration of selected major (Al, Ca, Fe, K, Mg, Na, P, Si, Ti) and minor elements (Ba, Co, Cr, Cu, Mn, Mo, Nb, Ni, Pb, Rb, Sr, V, Y, Zn, Zr). Precisions of the analyses (total rock) are ±3% for the major elements (except for Na which is ±7%) and ±5% for the minor elements (except for Pb which is ±8%). The concentrations of total sulphur, nitrogen and carbon were determined using a Carlo Erba® 1500 NCS analyzer. Mineralogy of bulk samples was resolved by X-ray diffractometry. Relative mineral abundances were estimated by ratioing the primary (characteristic) peak intensities of the major minerals.

For determination of $\delta^{13}C_{org}$ whole-rock samples were crushed and repeatedly treated with 50% HCl for 48 h, decanted, rinsed with deionized water and decanted. Crushed samples were left untreated for stable nitrogen isotope ratio determination of total nitrogen. Isotopic measurements for $\delta^{13}C_{org}$ were obtained using a Fisons NA 1500 CN analyzer coupled to a VG PRISM® mass spectrometer. The carbon dioxide gas was trapped on the mass spectrometer in liquid nitrogen, where a dual inlet allowed for determination of the relative isotopic difference ($\delta^{13}C_{org}$) between the reference gas and the sample gas. The ratio is reported in the conventional δ notation relative to the currently used Vienna Pee Dee Belemnite (VPDB), where the $\delta^{13}C_{org}$ for NBS 19 is +1.95‰ and for NBS 21 is -27.96 ± 0.02‰ ($n = 5$). For determining $\delta^{15}N_{tot.}$ the same instrumentation was used, but the set-up was changed for "continuous-flow" analyses where "atmospheric air" is reported as $\delta^{15}N = 0.00$‰ and a lab standard (acetanilide) was calibrated against air. Precisions for both $\delta^{13}C_{org}$ and $\delta^{15}N_{tot.}$ are ±0.2‰.

Polished pellets of kerogen concentrates and bulk rock samples orientated perpendicular to bedding were examined by incident and blue light excitation with an oil immersion 40× objective using standard coal petrographic techniques (Bustin et al., 1985). Point counting transects (350 points per sample) of whole rock samples were undertaken at orientations perpendicular to bedding.

Fourier transform infrared (FTIR) spectroscopy from select Exshaw and Big Valley samples was conducted on 29 KBr pellets of demineralized kerogen concentrates. Crushed whole-rock samples were repeatedly treated with 50% HCl for 48 h, decanted, rinsed with deionized water and decanted. Samples were then repeatedly bathed in 48% HF for 48 h, then decanted before being rinsed several times in deionized water and decanted again. Samples were subsequently oven dried at 40°C for 10 d. One mg of sample was ground and mixed with 190 mg of oven-dried (24 h at 200°C) KBr (i.r. grade), and pellets formed under 10,000 kg/cm^2 pressure and vacuum for 5 min. One sample was placed in an oven at 200°C for 48 h to determine the potential effects of oxidation during sample preparation.

The KBr pellets were analyzed on a Nicolet® 710 Fourier Transform-infrared spectrometer. Resolution was 8 cm^{-1} with an analytical range 400–4000 cm^{-1}. Background, blank reference pellets, and all samples were analyzed at 128 scans and co-added. Sample and reference pellets were ratioed to background noise. Intense absorption between 400 and 800 cm^{-1} may indicate the presence of pyrite and the incomplete removal of aluminosilicate clays. The coating of clay by amorphous organic matter (AOM) may have prevented complete aluminosilicate dissolution. All spectra are plotted in absorbance mode.

The KBr spectrum was subtracted from sample spectrum in order to remove pellet "noise" once baseline corrections had been made. Peak assignments for absorption bands (Table 5) were made according to Painter et al. (1981), Wang and Griffiths (1985) and Rochdi et al. (1991). Areas occupying spectral bands in the ranges 3000–2800 and 1800–1520 cm^{-1} were integrated and ratioed following baseline correction. The absorption bands in the range 3000–2800 cm^{-1} represent stretching aliphatic methyl and methylene groups, whereas the absorption bands in the range 1800–1520 cm^{-1} represent C=O (1710 cm^{-1}), ketone, amide or quinone (1650 cm^{-1}), C=C, C=O and COO– (1610 cm^{-1}) oxygen functional groups (Painter et al., 1981). The degree of kerogen oxidation can be determined by:

$$\text{Ox.I.} = \frac{\text{integrated area between 1800 and 1520cm}^{-1}\text{ bands}}{\text{integrated area between 3000 and 2800cm}^{-1}\text{ bands}}$$

as originally defined by Benalioulhaj and Trichet (1990), and modified by Tribovillard et al. (1992) and Tribovillard et al. (1994). The difference in relative intensities of the spectral absorbance bands reflects the amount of oxidation experienced by the organic matter (Tribovillard et al., 1994). Oxidation of organic matter

Table 5
Assignments of functional groups to spectra derived from FT-i.r. spectroscopy (Painter *et al.*, 1981; Rhoads *et al.*, 1983; Wang and Griffiths, 1985; Barakat *et al.*, 1990; Rochdi *et al.*, 1991; Mastalerz *et al.*, 1993). δ: deformation vibration; $\sqrt{}$: stretching vibration; as: asymmetric; s: symmetric; Peak intensity m: moderate; s: strong.

Function	Vibration mode	Peak (cm^{-1})	Integration range	Abbreviation
OH	νOH	3500–3000 (m)	3700–3100	νOH
	δOH (H_2O)	1630		
Aromatic CH	νCH ar.	~3050–3000	3100–3000	νCH ar.
	δCH ar. (1 adj. H)	~875		
	δCH ar. (2 adj. H)	~825	920–720	δCH ar.
	δCH ar. (4 adj. H)	~755		
CH_3	νas CH_3	~2960	3000–2800	νCH ali
	νs CH_3	~2870	2880–2820	νCH_3
	δas CH_3	~1475	1475–1390	δCH ali
	δs CH_3	~1380 (s)	1390–1300	δCH_3
CH_2	νas CH_2	~2920 (s)	3000–2800	νCH ali
	νs CH_2	~2850 (s)		
	δas CH_2	1475 (s)	1475–1390	δCH_2
C=O esters		~1745		
C=O carbonyl		~1710 (m)		
C=O carboxyl		~1710 (m)	1800–1520	C=O + C=C
C=O conjug. ketones		~1650 (s)		
C=C		~1610– ~ 1500	1520–1475	C=C
Pyrite		420 (s)		
Quartz		736/658 (s)		
C=O alcohols		1162 (m)	1170–1025	C=O
Tertiary		1083 (m)		
Secondary		1032 (m)		
Primary ethers	νC–O–C	1200–1040	1100–1000	C–O–CS

is recognized by a decrease in aliphatic band intensity and an increase in OH, C=C and C=O band intensities (Rochdi et al., 1991).

3. Geological setting and lithology

Devonian–Carboniferous strata of the Big Valley and Exshaw Formations were deposited in an epicontinental sea on the Alberta cratonic platform (Figs. 1 and 2). The AUCP was a broad platform on the western flank of the ancestral North American convergent continental margin (Richards, 1989), which passed westward into the Prophet Trough, a northerly extension of the Antler Foreland Basin in western United States (Richards, 1989). The Prophet Trough is bounded to the west by plutonic, volcanic and conglomeratic deposits of the pericratonic Kootenay Terrane (Gordey et al., 1987). Big Valley carbonates and Exshaw black mudrocks pass westward in the Prophet Trough to interbedded siltstones and dark-grey shales of the Besa River Formation (Pelzer, 1966; Richards, 1989).

Organic-rich mudrocks of the Exshaw Formation represent the culmination of a transgressive episode that began with deposition of Big Valley carbonates in the subsurface of Alberta and outcrops of the Rocky Mountains (Johnson et al., 1985; Meijer Drees and Johnston, 1993). The Big Valley carbonates transgressed across a regional unconformity surface capping the Stettler shallow marine carbonate ramp and evaporite accumulation (Meijer Drees and Johnston, 1993; Fig. 2). The latest Devonian transgressive episode led to the demise of the Big Valley carbonate ramp and subsequent deposition of Exshaw mudrocks (lithofacies B_1; Savoy, 1992; Caplan et al., 1996). A eustatic sea-level fall at the Devonian–Carboniferous (D–C) boundary (Sandberg et al., 1988) terminated deposition of organic-rich mudrocks (lithofacies B_1) and was followed by sedimentation of organic-lean mudrocks (lithofacies B_2) on the distal sediment-starved palaeocontinental shelf. Lithofacies B_2 mudrocks pass southeastward into calcareous siltstones and nearshore marine cross-bedded calcareous sandstones in the southeastern extremity of Alberta.

Samples from three lithofacies (B_{BV}, B_1 and B_2) representing contrasts of organic-richness were selected

from a cored interval (well 08-23-080-24W5) for geochemical and petrological characterization (Figs. 1 and 3; Tables 1–4). Lithofacies B_{BV} of the Big Valley Formation extends across the subsurface of northern and western Alberta. The lithofacies is composed of sharp-based, bioclastic, bioturbated carbonate grainstones interbedded with crinoidal mudstones and wackestones. Allochems include brachiopods, crinoid ossicles, bryozoa, ostracods, conodonts, in addition to phosphate and glauconite peloids. The absence of carbonate shoals within the lateral extent of Big Valley Formation suggests that these deposits had accumulated on a gently sloping carbonate ramp (Saller and Yaremko, 1994). Presence of sharp-based, bioturbated bioclastic grainstones implies reworking of the substrate by occasional storm waves (Meijer Drees and Johnston, 1993) under an oxygenated water column.

Lithofacies B_{BV} passes sharply up into black, laminated, organic-rich mudshales (laminated mudrock with appreciable silt content) of the Exshaw Formation (lithofacies B_1; Figs. 2 and 3). This lithofacies is laterally extensive throughout the subsurface of Alberta and outcrops in the Front Ranges of the Canadian Cordillera (Macqueen and Sandberg, 1970; Richards and Higgins, 1988; Savoy, 1992). These mudshales are composed of a laminated organic-clay matrix and discrete graded silt laminae. The frequency of silty laminae is highest at the top and bottom of the lithofacies. Radiolaria and sponge spicules occur in lithofacies B_1 as well as pyrite, phosphate and chert nodules. This lithofacies was deposited on the westward deepening palaeocontinental shelf of the Alberta cratonic platform (Savoy, 1992). The graded siltstone laminae provide evidence for sea floor reworking and sediment transport by waning, distal storm-generated currents in a benthic anoxic environment on the outer continental shelf.

Lithofacies B_1 is sharply overlain by grey-green, laminated, silty mudshales of lithofacies B_2 of the Exshaw Formation (Fig. 3). This lithofacies is restricted to the subsurface of northwestern Alberta and has been identified from outcrop sections at Jura Creek and Moose Mountain in the Rocky Mountain Front Ranges of western Alberta (the calcareous shale member of Richards and Higgins, 1988). Lamination and absence of biogenic activity in this lithofacies suggests that bottom waters above the sediment–water interface were anoxic. Occasional sharp-based, graded silty laminae record the rare influence of sea floor reworking by storm-generated currents. Lithofacies B_2 conformably passes up into bioturbated, calcareous siltstones of the Exshaw Formation. These siltstones have been interpreted as higher energy deposits influenced by more frequent storm-derived currents on an inner continental shelf setting, characterized by oxic bottom waters (Richards and Higgins, 1988; Savoy, 1992).

4. Results

4.1. Pyrolysis

Lithofacies B_{BV} contains low TOC (mean 0.22 wt%; standard deviation (S.D.) = 0.16 wt.%), HI values (mean 111 mg HC/g C_{org}; S.D. = 77 mg HC/g C_{org}; Tables 1–4, Fig. 4) and plots in the Type III/IV region of the modified Van Krevelen diagram. Lithofacies B_1 contains high TOC (mean 10 wt%; S.D. = 4.0 wt%) and has an average HI of 659 mg HC/g C_{org} (S.D. = 125 mg HC/g C_{org}; Fig. 4, Tables 1–4). Organic matter of lithofacies B_1 is Type I and I/II hydrogen-rich kerogen, probably derived from resistant organic tissues of cyanobacteria, phytoplankton or zooplankton (Fig. 5; Tissot and Welte, 1984). TOC and HI profiles vary erratically in lithofacies B_1 but there is an overall decrease upwards from 17.5 to 3 wt% TOC and in HI from 782 to 352 mg HC/g C_{org} (Fig. 4).

Lithofacies B_2 has an average TOC of 3 wt% (S.D. = 0.5 wt%) and HI of 372 mg HC/g C_{org} (S.D. = 81 mg HC/g C_{org}; Tables 1–4; Fig. 4). Organic matter is Type II/III kerogen (Fig. 5). Type III kerogen typically represents hydrogen-poor terrestrial material (Tissot and Welte, 1984), yet petrographic examination reveals no, or only rare quantities of, vitrinite group macerals. T_{max} values of kerogen from each lithofacies (ranging from 413 to 432°C) indicate that thermal maturity is below that of the oil window (Espitalié et al., 1977; Peters, 1986).

4.2. Inorganic geochemistry

Elemental concentration profiles through the Exshaw Formation qualitatively highlight subtle changes in the contribution of detrital input that is not readily distinguishable by visual examination alone. Elements that are enriched in detrital minerals include Ba, Cr, K, Na, Rb, Ti and Zr. The detrital-proxying nature of these elements is evident from their close association with Al (Tables 1–4), and from published accounts that describe their known geochemical association with detritus (e.g., Wedepohl, 1978). As aluminum is only known to occur in aluminosilicates, the element/Al ratio can be used to qualitatively estimate the contribution of elemental concentrations from a non-aluminosilicate source or a variable detrital mineralogy (Calvert, 1990).

Element/Al ratios for Ti, K, Si and Zr decrease slightly upward from lithofacies B_1 into lithofacies B_2 (Fig. 6), whereas ratios of Na, Rb and Ba to Al increase upward. The quartz/clay ratio (determined from counts of representative peaks for quartz and clays on the XRD spectra) is higher in lithofacies B_1 than lithofacies B_2. There is no clear trend in the ratio

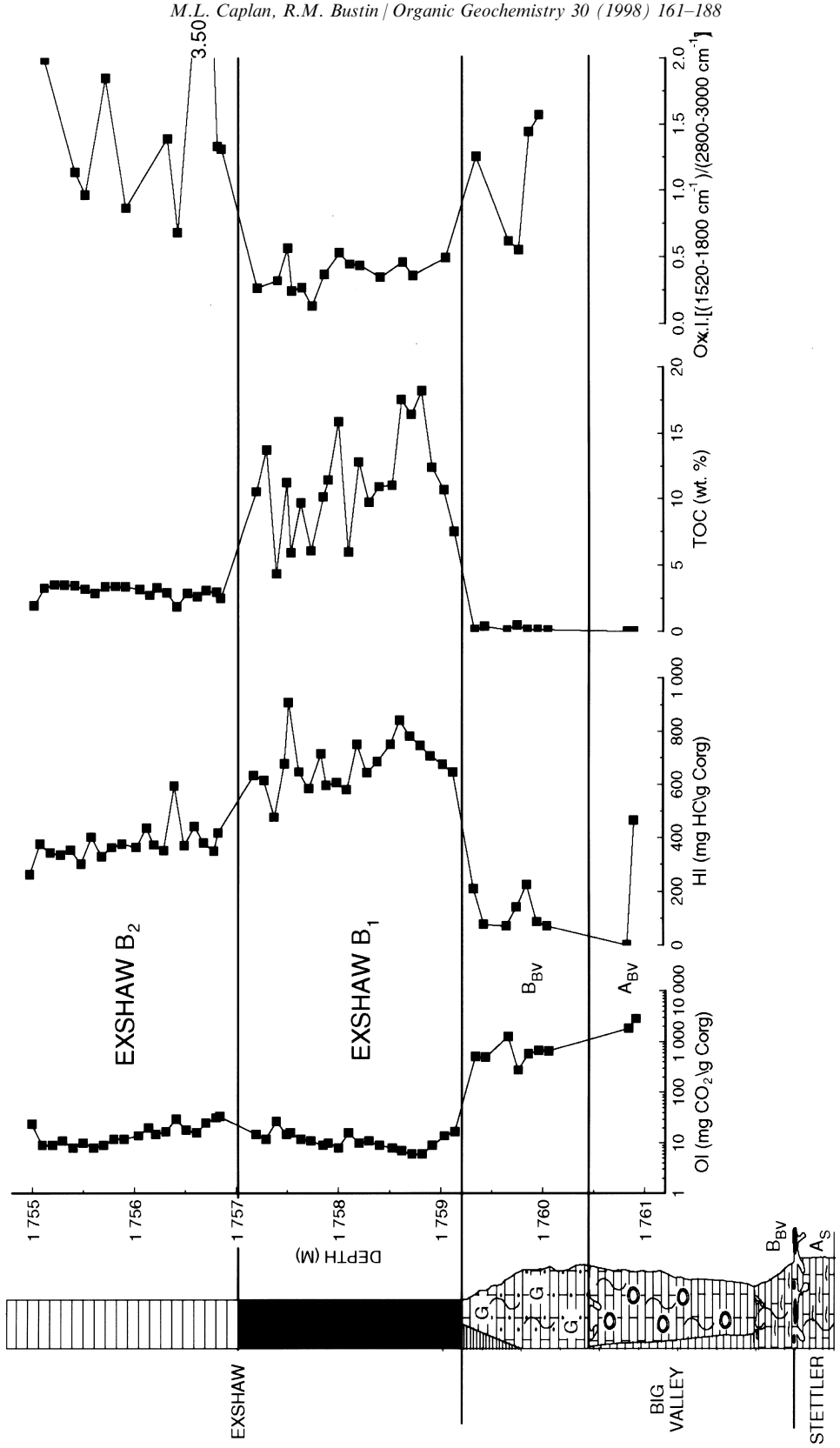

Fig. 4. Vertical profile of geochemical (pyrolysis and FTIR) parameters through the cored interval of well 08-23-080-24W5; including oxygen index (OI), hydrogen index (HI), total organic carbon (TOC) from bulk samples and the oxidation index (Ox.I.) from concentrated kerogens.

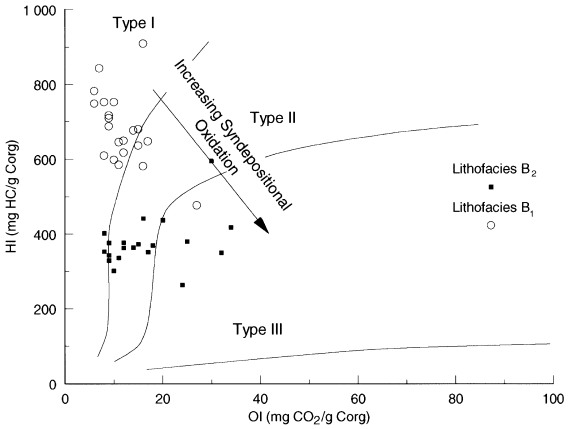

Fig. 5. Modified Van Krevelen diagram of HI vs. OI for bulk samples from lithofacies B_1 and B_2. Big Valley samples have very low TOCs and HI, but extremely high OIs (off the scale). Trends from high HI, low OI to low HI, high OI is interpreted as the effects of increased syndepositional oxidation of organic matter (well 08-23-080-24W5).

of quartz to clays through lithofacies B_1 (ranging from 3.3 at the base to 6 at the top), and a fluctuation in ratio from 2.6 to 3.7 throughout lithofacies B_2 (Fig. 6).

Slight decreases in K, Si, Ti and Zr to Al and quartz to clay ratios from lithofacies B_1 to lithofacies B_2 indicate subtle differences in both mineralogy and grain size (Fig. 6). Titanium and Zr-bearing accessory minerals typically occur in sandy strata (Calvert, 1976). Higher Ti and Zr/Al ratios may indicate the presence of small quantities of accessory minerals associated with laminae of sand- and silt-sized particles in lithofacies B_1. The higher abundance of sand- and silt-sized quartzose laminae in lithofacies B_1 is supported by the high silica/Al and quartz/clay ratios that decrease into lithofacies B_2.

Vertical concentration profiles of Cr, Mn, Mo and V to Al ratios through the Big Valley and Exshaw mudrock lithofacies demonstrate enrichments in lithofacies B_1 (Tables 3–4; Fig. 7), and a good correlation between TOC and Mo suggests a close affinity of Mo to kerogen. Cr, Mo and V are typically enriched in black shales and Recent anoxic sediments (Vine and Tourtelot, 1970; Calvert and Pedersen, 1993). The high ratios of these elements in lithofacies B_1 indicate that the sediments and/or benthic waters at the time of deposition were probably anoxic. The ratios are lower in lithofacies B_2, but nonetheless, significantly higher than for B_{BV}, suggesting a continuation of benthic anoxia. Cr and V may have been adsorbed on particle surfaces under low redox conditions, whereas Mo may have been directly incorporated into the kerogen or precipitated with sulphides (Bertine, 1972; Ripley et al., 1990). Manganese/Al ratios are much higher in Big Valley lithofacies than either lithofacies B_1 or B_2, and are positively correlated with Ca. Manganese is typically enriched in carbonates deposited under oxygenated bottom waters (Calvert and Pedersen, 1996), however reduced forms of Mn in anoxic waters form soluble phases, and are represented by lower concentrations in the underlying sediments. The reversed association between the Mn/Al ratio and Cr/Al, Mo/Al and V/Al from the three lithofacies indicates that bottom waters were more likely oxygenated during deposition of organic matter of the Big Valley than for either lithofacies B_1 and B_2. Variations of these ratios between lithofacies B_1 and B_2 may suggest a contrast in the affinity of these elements to organic matter, or an increase in degradation and consequent liberation of the elements from oxidized organic matter in the water column.

4.3. Organic petrography

Lithofacies B_{BV}, B_1 and B_2 contain similar maceral assemblages. Due to the very small sample size, organic matter from lithofacies B_{BV} could not be quantified (Figs. 8 and 9). All lithofacies exhibit, in decreasing order of abundance, matrix-bound bituminite, disseminated alginite, liptodetrinite, inertodetrinite and vitrodetrinite. Alginite comprises thick- and thin-walled *Tasmanites* praesinophytes and *Leiospheres*. In blue light, alginite macerals range from yellow-green discrete bodies to reddish-brown diffuse material that, in places, grade into matrix-bound bituminite. Pyrite framboids are ubiquitously associated with alginite macerals. Bituminite typically exhibits yellow-green fluorescence and is intimately associated with the clay matrix. Bituminite locally contains yellow to red fluorescing liptodetrinite, which is more abundant and occurs as discrete layers at the base of lithofacies B_1 (Figs. 8 and 9). Layers of vitrodetrinite and angular inertodetrinite particles are common in laminae from the basal parts of lithofacies B_1, but are rarer in lithofacies B_{BV} and B_2. Lithofacies B_1 and B_2 are dominated by marine liptinite macerals (Fig. 8), although within discrete silty laminae terrestrially-derived vitrodetrinite, inertodetrinite and reworked marine liptodetrinite are more abundant (Fig. 8).

4.4. $\delta^{13}C_{org}$ and $\delta^{15}N_{tot}$ stable isotopes

Average stable carbon isotope ratios of bulk organic carbon ($\delta^{13}C_{org}$) for lithofacies B_{BV} are −27.3‰, with values ranging from −26.9‰ to −27.5‰ (Table 1; Fig. 10(a)). The average $\delta^{13}C_{org}$ for lithofacies B_1 is −28.2‰, with values ranging from −27.8‰ to −28.5‰. In lithofacies B_2 the average $\delta^{13}C_{org}$ is −28.5‰, with values ranging from −28.2‰ to −28.8‰ (Table 1, Fig. 10(a)). Within lithofacies B_{BV}, $\delta^{13}C_{org}$ values become lighter as the Exshaw–Big Valley contact is

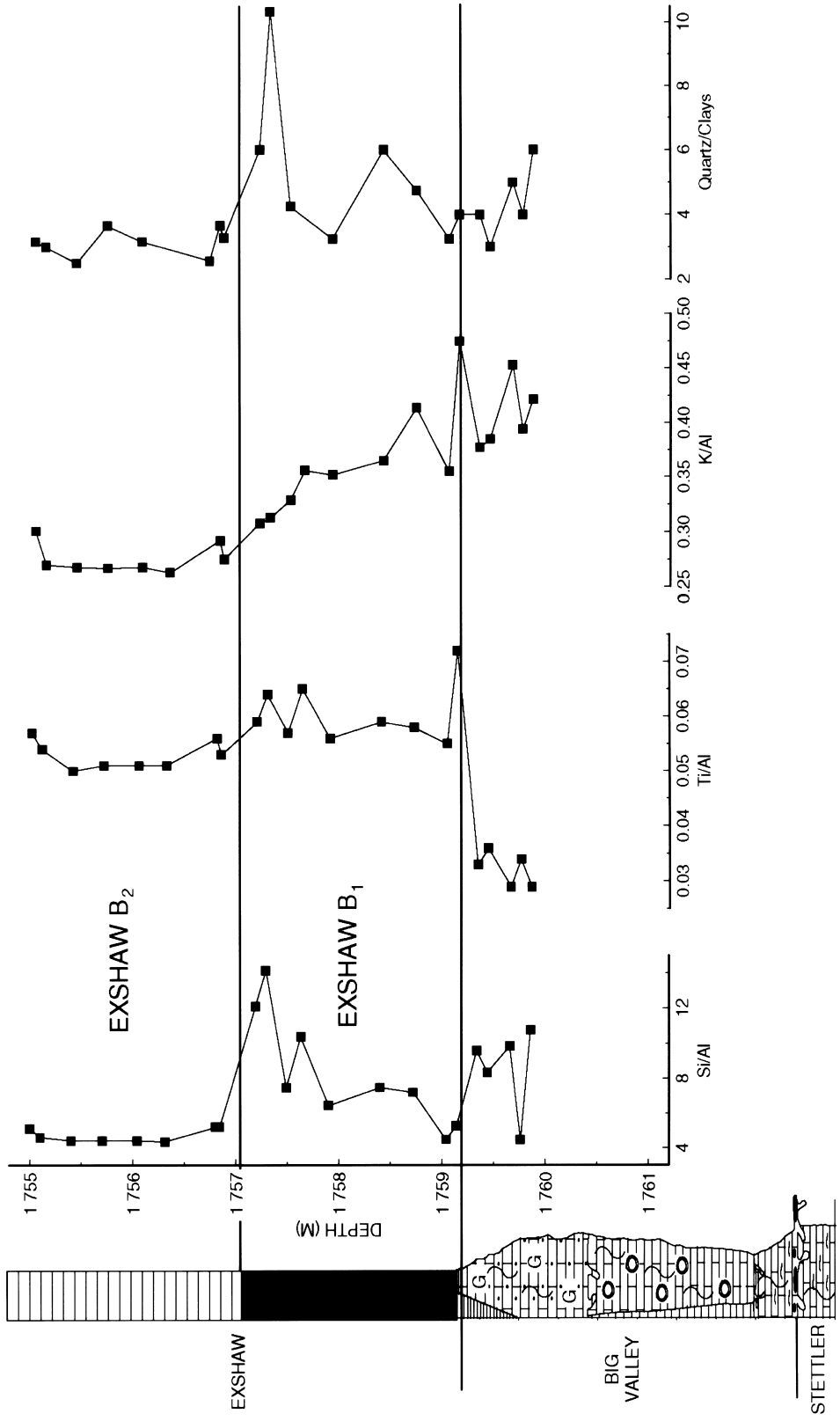

Fig. 6. Vertical profile of detrital-proxying elements and plots of relative granulometric variations up core. Depth against Si/Al, Ti/Al, K/Al and quartz/clays for lithofacies B_{BV}, B_1 and B_2 for well 08-23-080-24W5.

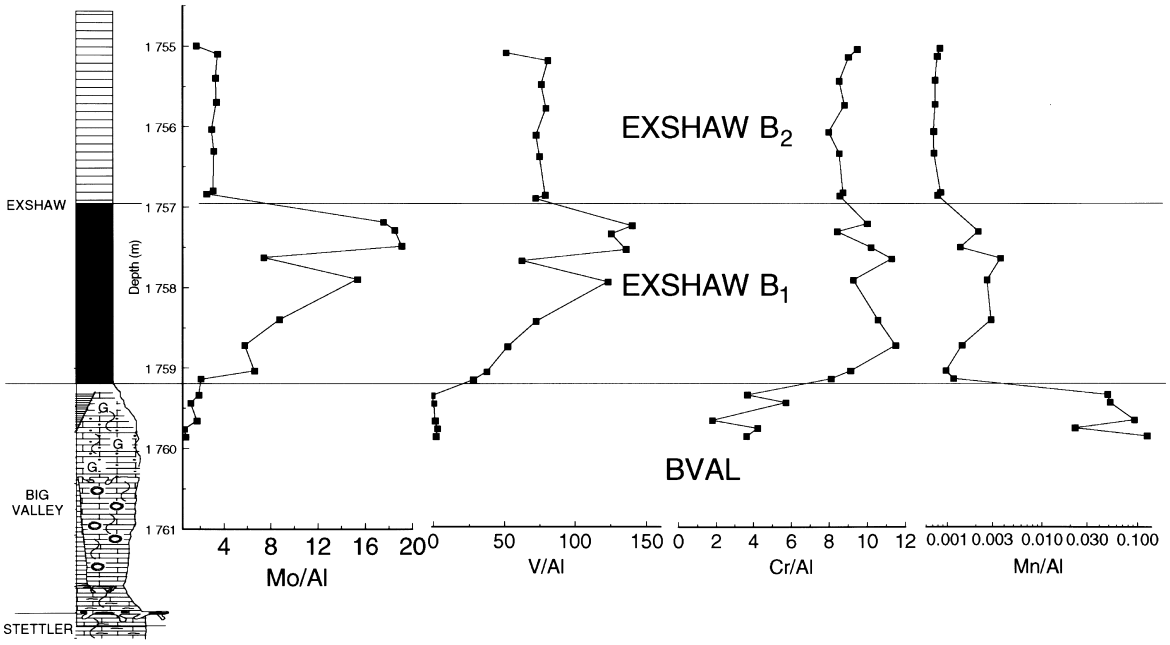

Fig. 7. Vertical profile of Cr/Al, Mn/Al, Mo/Al and V/Al through lithofacies B_{BV}, B_1 and B_2 for well 08-23-080-24W5.

approached. Profiles of $\delta^{13}C_{org}$ display a gradual trend toward lighter values from lithofacies B_1 to B_2.

Bulk rock nitrogen isotopes are thought to closely represent those values expected from organic nitrogen in organic-rich facies (Calvert et al., 1996). The very good correlation between TOC and total nitrogen contents, and the very small intercept (Fig. 10(b)), imply that most of the nitrogen in lithofacies B_{BV}, B_1 and B_2 resides in organic matter. Very similar $\delta^{15}N_{tot}$ and $\delta^{15}N_{org}$ values derived from correlative strata of the D–C New Albany Shales in New York State (Calvert et al., 1996) indicate that, in organic-rich facies, $\delta^{15}N_{tot}$ results are comparable to $\delta^{15}N_{org}$ values. Average values of $\delta^{15}N_{tot}$ for lithofacies B_{BV} are 1.6‰, 0.1‰ for lithofacies B_1 and 1.8‰ lithofacies B_2 (Table 1). $\delta^{15}N_{tot}$ values become progressively lighter approaching the Big Valley to Exshaw contact, they are lightest in lithofacies B_1 and exhibit an abrupt 1.7‰ shift to heavier values in lithofacies B_2 (Fig. 10(a)).

4.5. Fourier transform infrared (FTIR) spectroscopy

FTIR spectra of representative powdered kerogen concentrate from each lithofacies exhibit subtle variations in form (Fig. 11; Table 5). High aliphatic, low aromatic and variable oxygenated functional group band intensities from spectra derived from the Exshaw samples rich in alginite and bituminite are similar to spectra determined from *Tasmanites* macerals by other workers (e.g. Lin and Ritz, 1993a,b). A strong absorption peak at 1650–1600 cm^{-1} is interpreted as conjugated ketones (Rhoads et al., 1983; Mastalerz et al., 1993). Other organic compounds proposed to represent this band including amides (Dyrkacz et al., 1984, Derenne et al., 1991) and aromatics (Painter et al., 1981; Wang and Griffiths, 1985; Rochdi et al., 1991). Low nitrogen contents (less than 0.6%) from lithofacies B_1 and B_2 suggest that amides do not contribute to the 1650–1600 cm^{-1} band, and the very minor amounts of inertinite and vitrinite present preclude the band as only representing aromatic carbon.

Subtle, but important, chemical contrasts in the kerogen concentrates from lithofacies B_{BV}, B_1 and B_2 are revealed by semi-quantitative analysis of FTIR spectra (Fig. 11). Oxidation experiments of organic matter report an increase in ether, carbonyl, carboxyl, quinone and ketone oxygen functional groups at the expense of hydrogen-rich aliphatics (Calemma et al., 1988; Kister et al., 1988; Barakat et al., 1990; Rochdi et al., 1991; Tognotti et al., 1991). The FTIR-derived oxidation index (Ox.I.) is a semi-quantitative measure of degree of organic matter degradation from the analysis of various organic components of a kerogen (Benalioulhaj and Trichet, 1990). The oxidation index is defined as the ratio of the integrated band areas representing oxygen functional groups (1800–1520 cm^{-1}) to the aliphatic band areas (3000–2800 cm^{-1}). Low Ox.I. values are interpreted as indicating a greater degree of organic matter preservation (reflected by higher content of hydrogen-rich organic

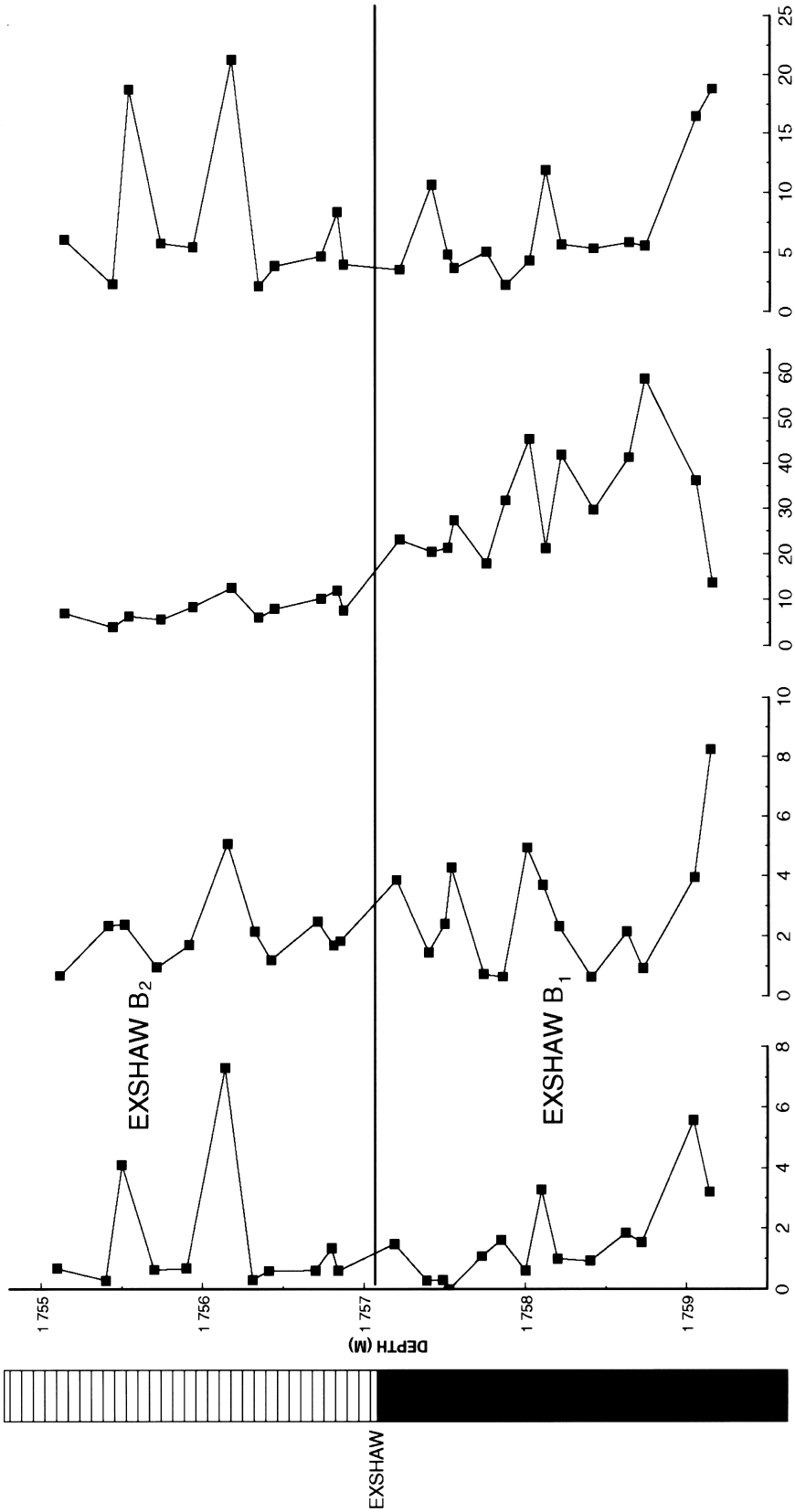

Fig. 8. Profile of maceral type volumetric abundance through Exshaw lithofacies B_1 and B_2 of well 8-23-080-24W5.

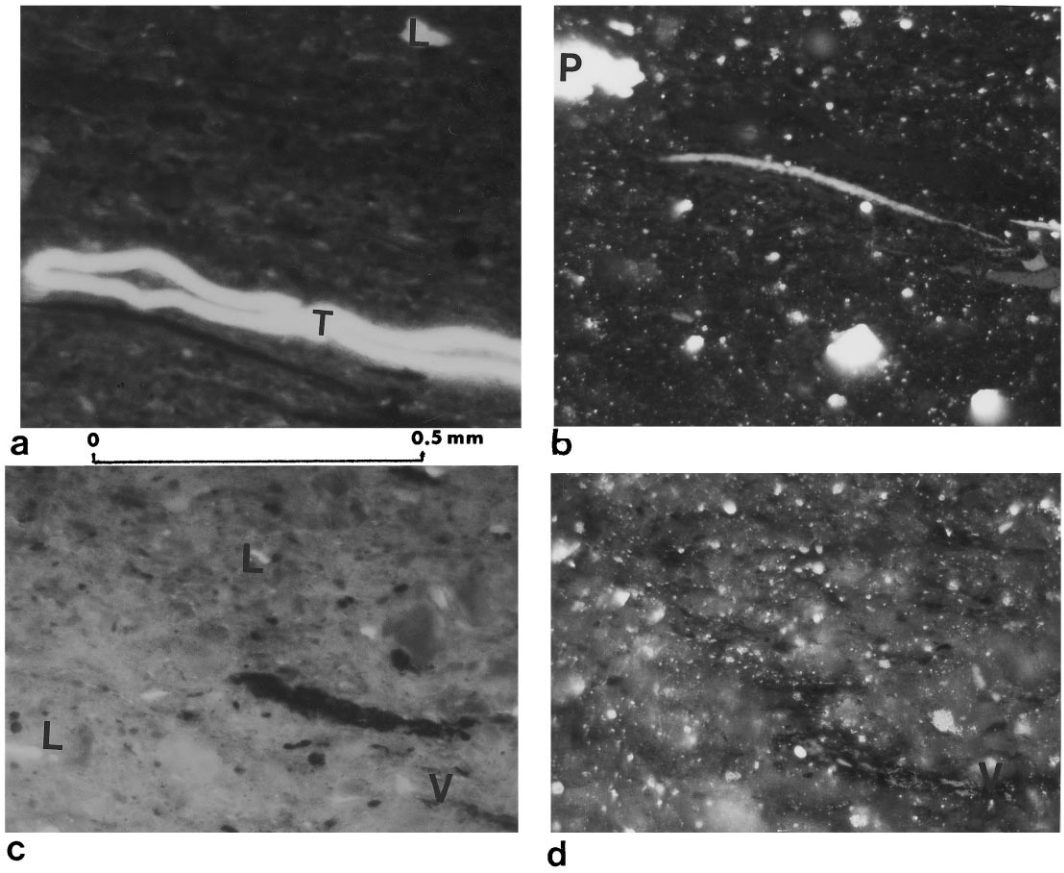

Fig. 9. Photomicrographs of characteristic organic matter found in lithofacies B_1 and B_2 taken under oil immersion 40× magnification objective: (a) thick-walled *Tasmanites* (T) and liptodetrinite (L) matrix material from lithofacies B_1, sample #24 in blue light; (b) sparse vitrinite macerals and disseminated pyrite crystals (P), sample #24 in reflected light; (c) common liptodetrinite (L) particles and non-fluorescing vitrinite (V) from lithofacies B_2 in blue light, sample #15; (d) rare vitrinite (V) maceral with black rim reflecting partial oxidation from lithofacies B_2, reflected light, sample #15. Scale bar identical for each shot at 500 μm.

compounds and lower content of oxygen functional groups), whereas high Ox.I. reflects advanced stages of oxidation (lower content of hydrogen-rich organic compounds and higher content of oxygen functional groups). Systematic variations of the Ox.I. occur between each lithofacies (Table 1; Fig. 5). The average Ox.I. for lithofacies B_{BV} is 1.09, 0.38 for lithofacies B_1 and 1.5 for lithofacies B_2. Lithofacies B_{BV} and B_2 display a strong absorbance of the alcohol, ether and 1600–1650 cm^{-1} bands, whereas lithofacies B_1 is characterized by weak absorbance of the alcohol, ether and 1600–1650 cm^{-1} bands and stronger absorbance of the aliphatic stretching and methyl deformation bands (Fig. 11). The oxidation index (Ox.I.) shows a poor negative correlation with HI, HI*, TOC and a good positive correlation with $\delta^{15}N_{tot}$ (Fig. 12). HI* is defined as the hydrogen index of concentrated kerogen samples pyrolyzed after HF acid treatment. There is no correlation between Ox.I. and $\delta^{13}C_{org}$.

5. Discussion

The TOC content, HI and Ox.I. of organic-rich sedimentary facies can be influenced by sedimentation rate, degree of microbial oxidation, organic matter source type and supply of organic matter (e.g. Demaison and Moore, 1980; Calvert, 1987; Tyson, 1987, 1995; Pedersen and Calvert, 1990). Contrasting geochemical signatures of kerogen imply that differing palaeoceanographic processes influenced deposition of lithofacies B_{BV}, B_1 and B_2. Kerogen HI and OI (derived from pyrolysis) of organic-rich sedimentary facies are affected by the relative contributions of marine, terrestrial and degraded organic matter (Tissot and Welte, 1984). The change from Type I kerogen in lithofacies B_1 to Type II/III kerogen in lithofacies B_2 is not attributable to the effect of differing organic matter source as both lithofacies contain similar abundances of vitrodetrinite and inertodetrinite macerals (Fig. 8). Carbon isotopes of organic matter can delineate mod-

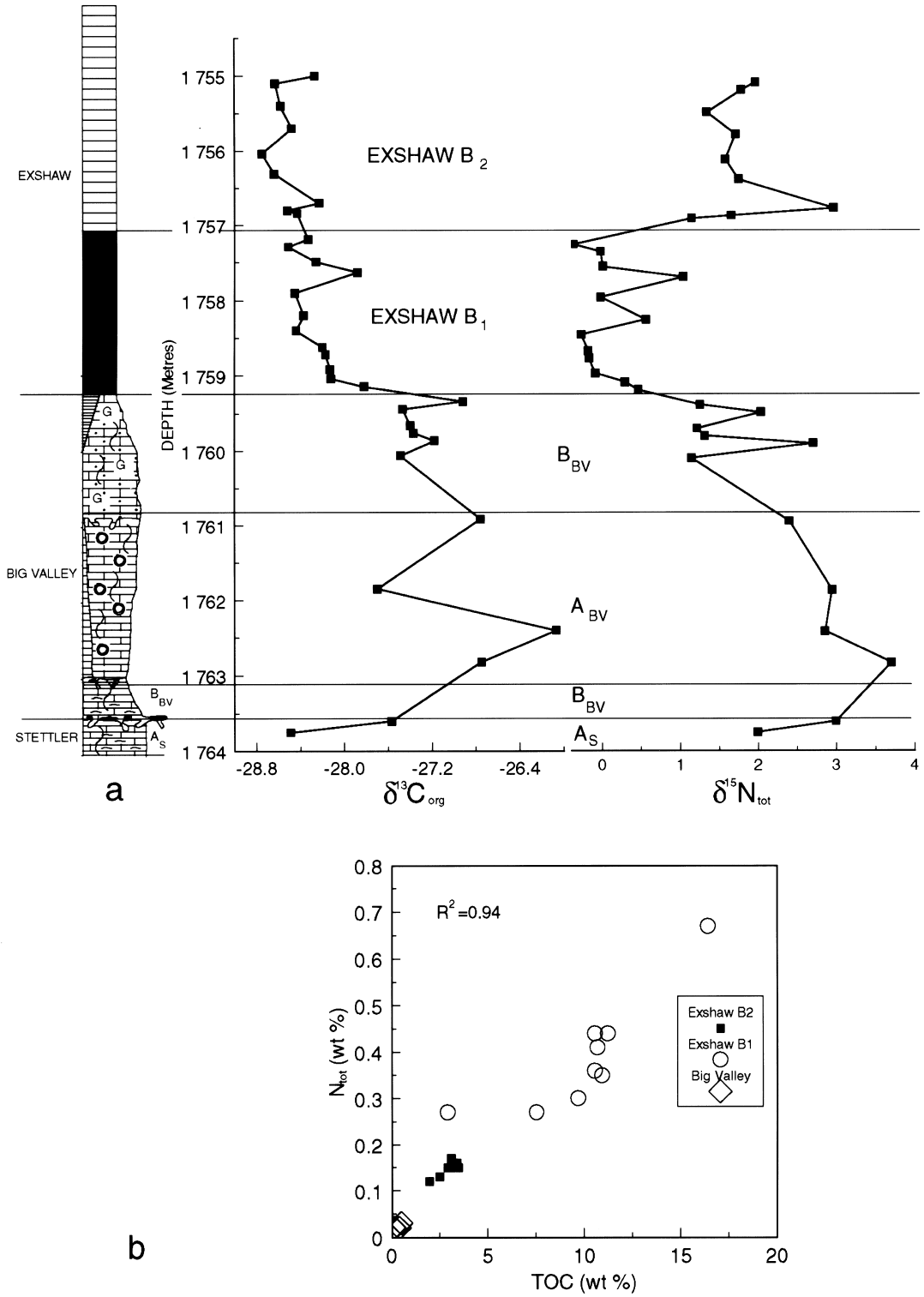

Fig. 10. (a) Vertical profile of stable isotopes of bulk organic carbon and total nitrogen from the Exshaw and Big Valley Formations; (b) scatter diagram showing positive correlation between TOC and total nitrogen content (well 08-23-080-24W5).

ern terrestrial (−26‰) from marine (−20‰) organic matter (Libes, 1992). However, Maynard (1981) and Calvert et al. (1996) observed the opposite isotopic signatures for marine (−30‰) and terrestrial (−26‰) kerogen from the Upper Devonian New Albany Shales. Calvert et al. (1996) explained such isotopic differences as reflecting a high partial pressure of atmospheric CO_2 during the Upper Devonian. Based on their hypothesis, the lighter $\delta^{13}C_{org}$ from lithofacies B_2 should indicate a greater relative input of marine organic matter than in lithofacies B_1. Applied to the Exshaw, these conclusions are inconsistent with the pyrolysis (Fig. 5) and petrographic analyses (Figs. 8 and 9). Petrographic analysis reveals that source type fluctuations can be ruled out as a factor controlling the HI variability between lithofacies B_{BV}, B_1 and B_2 kerogen. Factors other than organic matter source must be considered responsible for the contrasting geochemical characteristics of the Exshaw mudrock lithofacies. The roles of anoxia, grain size variation, organic matter reworking and organic matter supply are considered in the following sections.

5.1. Bottom water anoxia

From experimental work conducted by Jørgensen (1982) it was concluded that the rate and amount of microbial aerobic and anaerobic (excluding methanogenic diagenesis) degradation of organic matter is equal within anoxic and oxic environments. In addition, Cowie and Hedges (1992) demonstrate that biochemical constituents of organic matter exposed to oxic and anoxic bottom waters display no detectable geochemical differences. However, the presence of macrobenthos in modern and ancient oxic marine environments appears to enhance the efficiency of organic matter degradation (by reducing HI and TOC while increasing the OI) perhaps through the more efficient irrigation and circulation of dissolved oxygen through the bioturbated sediments (Demaison and Moore, 1980; Pratt, 1984). Applied to lithofacies B_{BV} of the Big Valley Formation, kerogen derived from the bioturbated carbonates displays high Ox.I. and OI, low HI and TOC which is interpreted to reflect the oxidative effects of macrobenthos-induced irrigation and oxidation of the organic matter. In contrast, variations of these geochemical parameters in laminated lithofacies B_1 and B_2 cannot be explained by variations in bottom water oxygen content or biogenic irrigation as both lithofacies are laminated and contain enriched concentrations of the "anoxia-proxying" elements Cr, Mo and V. Other processes better explain the contrasting quality and quantity of organic matter exhibited by these two lithofacies.

5.2. Grain size effects

Grain size changes can exert strong controls over total organic carbon content of sedimentary facies (Trask, 1939; Ibach, 1982; Tyson, 1987). Higher organic matter contents occur in clay-sized than silt- and sand-sized sediments from the modern continental margin (Trask, 1939). However, in the Exshaw mudrocks, organic matter contents are higher in lithofacies B_1 than lithofacies B_2 even though Cr, K, Si, Ti and Zr contents and quartz/clay ratios are higher in lithofacies B_1 than lithofacies B_2 indicating a slightly coarser grain size (Fig. 6). Grain size change thus does not appear to account for the decrease in organic matter quantity and quality displayed by lithofacies B_2.

5.3. Reworked organic matter

TOC and HI can be altered by the degree of organic matter reworking and benthic transportation into the depositional environment. Organic matter from coarser grained winnowed sediments of the modern Oman Margin record a decrease in TOC, HI and increase in C/N (Pedersen et al., 1992) interpreted as indicating the preferential degradation of more labile organic compounds during reworking. In such settings, aerobic oxidation of labile marine algal components and subsequent transportation by benthic currents may chemically alter the organic matter (decreasing HI), lead to its destruction (reduction of TOC) and significantly reduce its hydrocarbon potential (Huc et al., 1992; Pedersen et al., 1992). Similarly, towards the base and top of lithofacies B_1 silty laminae contain abundant liptodetrinite particles of reworked alginite bodies, which exhibit lower HI and TOC values. These laminae are interpreted as reflecting periods during which there was a marked increase in benthic transport, reworking and degradation of organic matter. The lower TOC and HI values for organic matter of lithofacies B_2 cannot be explained by reworking, as silty laminae and liptodetrinite macerals are rare compared to the lower parts of lithofacies B_1. Organic matter reworking by benthic transportation was probably more frequent in lithofacies B_1 and cannot be responsible for the observed geochemical contrasts in kerogen from lithofacies B_1 and B_2.

5.4. Variations in primary production

Oligotrophic and eutrophic regions of the Earth's oceans reflect strong differences in physical circulation, chemical and biological cycling of organic matter, which may be recorded by variations in the geochemical signatures of sedimented organic matter (e.g., Knauer et al., 1979; Demaison and Moore, 1980; Calvert, 1987; Pilskaln and Honjo, 1987). The degree

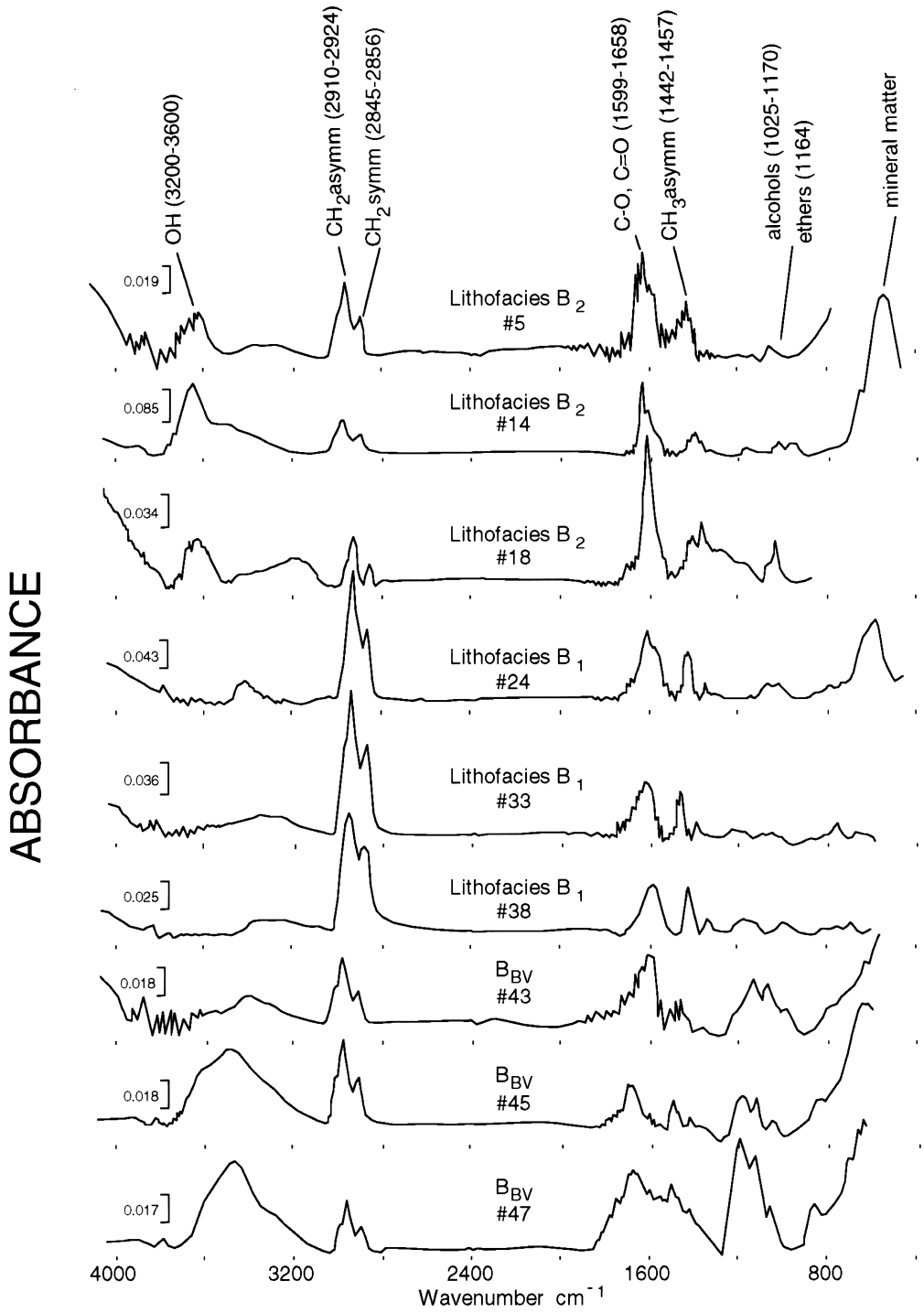

Fig. 11. Representative FTIR interferograms of kerogen concentrates from each of the lithofacies in well 08-23-080-24W5. Note consistently high absorbance at the 1625–1655 cm^{-1} band in all samples, systematic variation in aliphatic (2800–3000 cm^{-1}) and alcohol/ether (100–1170 cm^{-1}) absorbance bands. Distribution of absorbance peak or band indicated in parentheses.

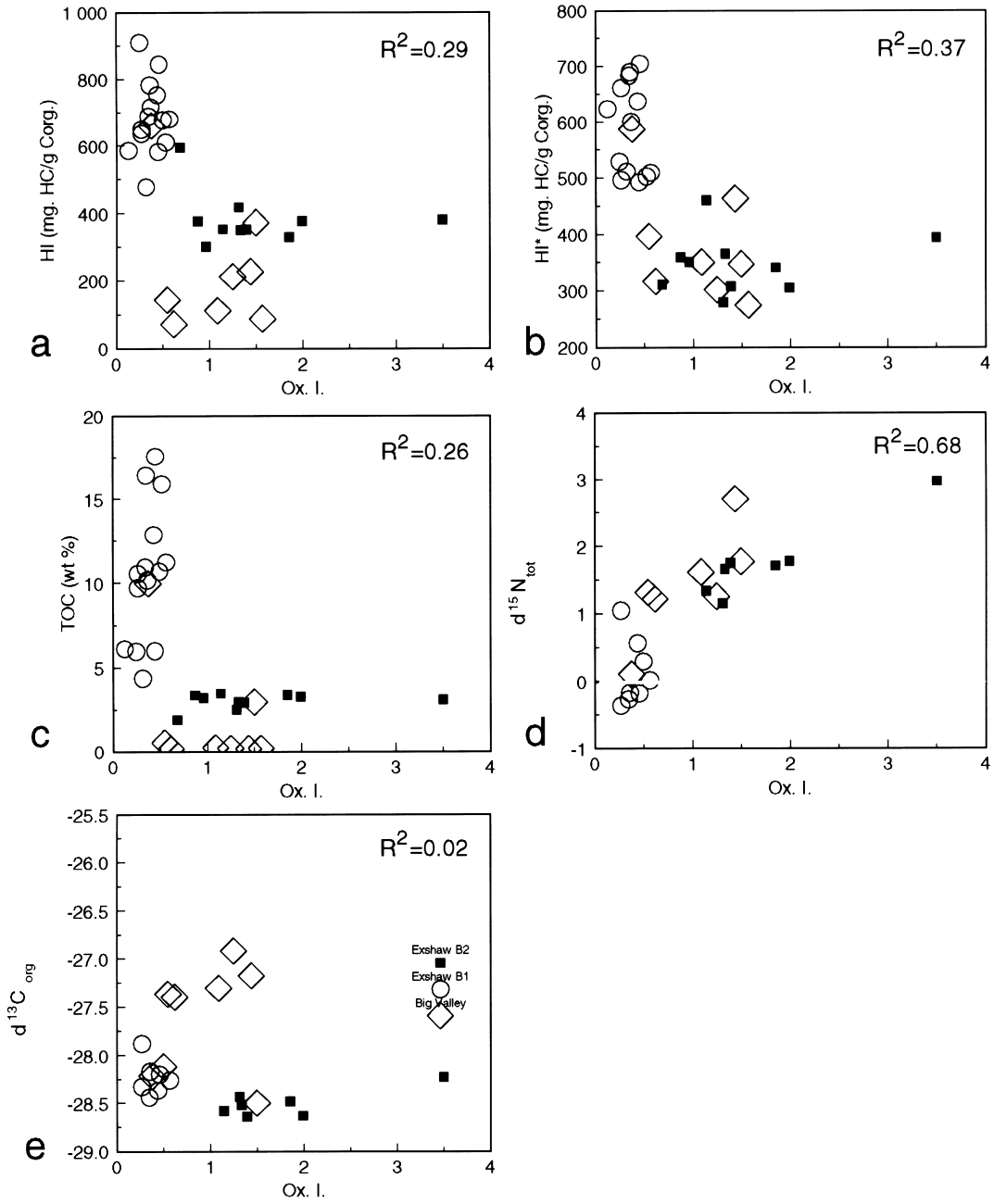

Fig. 12. FTIR and pyrolysis geochemical parameters and associations for: (a) HI vs. Ox.I.; (b) HI* and Ox.I.; (c) TOC and Ox.I.; (d) $\delta^{15}N_{tot}$ and Ox.I.; and (e) $\delta^{13}C_{org}$ and Ox.I.

of organic matter and nutrient recycling in the euphotic zone is governed by the ratio of new (nutrient input into the euphotic zone) to regenerated production (reutilization of nutrients from within the euphotic zone; Eppley and Peterson, 1979), this ratio rising in eutrophic regions. Eutrophic conditions lead to higher primary production, lower recycling of organic matter and greater export of organic carbon to deeper waters either as intact phytoplankton, encapsulated in zooplankton faecal material or as transparent exopolymer particles (TEP) and vegetative cell aggregates (Eppley and Peterson, 1979; Suess, 1980; Libes, 1992; Grimm

et al., 1997). Eutrophic environments tend to be characterized by larger, denser faecal pellets which sink at faster rates than smaller, less dense faecal pellets that typify oligotrophic environments (Pilskaln and Honjo, 1987). As a result, a high proportion of fresh, labile organic matter, with higher N:C and P:C ratios can be sedimented beneath modern upwelling cells (Porter, 1976; Eppley and Peterson, 1979; Knauer et al., 1979; Müller and Suess, 1979; Pilskaln and Honjo, 1987; Calvert and Pedersen, 1992). Suess and Müller (1980) have determined, based on sediment trap data from the open ocean, that only 20% of organic matter produced in the surface waters should be found below 175 m water depth in an oxygenated water column. Suess (1980) and Betzer et al. (1984) recognized that organic carbon flux in the water column was directly proportional to the primary productivity of surface waters, indicating that less organic matter is exported from the euphotic zone during oligotrophic conditions. The transit of more organic matter from the euphotic zone during high rates of primary production may reflect a decrease in the efficiency of organic matter grazers in the euphotic zone.

Conditions of water column eutrophy and oligotrophy, and the effects of this chemical change on the level of primary production and degree of organic matter recycling can be demonstrated by geochemical contrasts (TOC, HI, Ox.I., $\delta^{15}N_{tot}$ and $\delta^{13}C_{org}$) of kerogen from the Big Valley–Exshaw interval. A qualitative measure of nutrient addition to, and biological utilization within, the euphotic zone is given by $\delta^{15}N$ values (Altabet and Francois, 1994a,b; Montoya, 1994; Farrell et al., 1995). Altabet and Francois (1994a,b) observed a negative association between nitrate concentration in the euphotic zone and $\delta^{15}N_{org}$ values across a transect of the eastern Pacific equatorial upwelling cell. In eutrophic areas where nitrate stock in the euphotic zone is high, large isotope fractionation of nitrogen is caused by the preferential utilization of the lighter nitrogen isotope by phytoplankton. In oligotrophic regions where nutrient content in the euphotic zone is low, phytoplankton discrimination for the lighter nitrogen isotope diminishes, leading to heavier nitrogen isotope incorporation. Lighter $\delta^{15}N_{org}$ values appear to imply a high physical supply of nutrients relative to biological utilization. Heavier $\delta^{15}N_{org}$ values indicate a larger drawdown of a limited supply of nitrate in the euphotic zone, which results in isotopically heavy nitrogen in phytoplankton (Altabet and Francois, 1994a,b). Calvert et al. (1992b) who examined the geochemistry of ten sapropels recovered from Black Sea cores reached similar conclusions. They recognized that at high TOCs, sapropels exhibited very light $\delta^{15}N$, and they interpreted these geochemical signatures to represent formation of the sapropels during periods of eutrophication, enhanced primary productivity and high supply of organic matter to the sediment–water interface.

Applied to the Exshaw mudrocks, $\delta^{15}N_{tot}$ is negatively associated with TOC, where organic-lean lithofacies B_2 exhibits heavier $\delta^{15}N_{tot}$ values than organic-rich lithofacies B_1 (Fig. 10(a)). These results may indicate that organic matter of lithofacies B_2 accumulated during relatively more oligotrophic conditions than for lithofacies B_1. If nutrient concentrations and primary production of the water column did indeed vary between deposition of lithofacies B_1 and B_2, organic matter may have been exposed to varying degrees of recycling and oxidation in the water column.

The quality of organic matter preservation is demonstrated by the HI, Ox.I. and $\delta^{13}C_{org.}$ geochemical parameters. The Oxidation Index (Ox.I.) has been used as a proxy for organic matter oxidation (Benalioulhaj and Trichet, 1990; Tribovillard et al., 1992, 1994). Geochemical changes to incrementally oxidized organic matter have been observed experimentally (e.g. Barakat et al., 1990). These results demonstrate an increase in oxygen functional groups at the expense of aliphatics as kerogen and coal become progressively exposed to aerobic oxidation (Calemma et al., 1988; Kister et al., 1988; Barakat et al., 1990; Rochdi et al., 1991; Tognotti et al., 1991). Results from FTIR interferograms and Ox.I. from the Exshaw kerogen samples indicate that organic matter may have been exposed to varying degrees of oxidation. Kerogen samples from organic-lean lithofacies B_2 and B_{BV} show higher intensity peaks of oxygenated functional groups and hydroxyl bands at the expense of hydrogen-rich aliphatic compounds (higher Ox.I.) compared to kerogen derived from organic-rich lithofacies B_1 (Figs. 3 and 11), which may reflect an increase of organic matter oxidation.

$\delta^{13}C_{org}$ values have also been used as a proxy for organic matter oxidation (Tyson, 1995 and references therein). $\delta^{13}C_{org}$ values can, however, be affected by organic matter type, oxidation, and partial pressures of atmospheric and water column CO_2 (Libes, 1992; Rau, 1994). These processes can be ruled out as the slightly lighter $\delta^{13}C_{org}$ values in lithofacies B_2 (Fig. 10) could reflect a greater supply of terrestrial organic matter, yet vitrinite maceral content does not increase compared to lithofacies B_1. Increased partial pressure of atmospheric CO_2 can also produce lighter $\delta^{13}C_{org}$ isotope ratios, yet estimations of the atmospheric CO_2 content by Berner (1994) suggest a rapid decline at the Devonian–Carboniferous (D–C) boundary, as does the identification of glaciogenic diamictites from Gondwana (Caputo and Crowell, 1985) and heavier $\delta^{18}O_{carbonate}$ isotopes at the D–C boundary (Popp et al., 1986), all of which may indicate a cooler climate and decreasing atmospheric CO_2 content. The lighter $\delta^{13}C_{org}$ isotope ratios for lithofacies B_2 may alterna-

tively suggest selective organic matter degradation. Recent studies of organic matter oxidation show a more pronounced negative shift in $\delta^{13}C_{org}$ for oxic compared to anoxic water masses (Tyson, 1995, p. 409) and sediments (McArthur et al., 1992). McArthur et al. (1992) discovered that there was a 0.3–2.5‰ shift to lighter $\delta^{13}C_{org}$ values from oxic to nitrate-reducing zones in recent turbidites off Madeira reflecting the geochemical response to organic matter oxidation in the sediments. Redox sensitive $\delta^{13}C_{org}$ values are thought to reflect preferred liberation of more labile organic compounds (proteins and carbohydrates), that are isotopically heavy, leaving refractory organic matter enriched in isotopically light lipids (see Tyson, 1995, p. 409) during organic matter remineralization in the water column or sediments. Thus, the lighter $\delta^{13}C_{org}$ values in lithofacies B_2 compared to B_1 (Fig. 10) are tentatively interpreted to reflect a greater degree of oxidation of labile organic compounds either in the water column during periods of high organic matter recycling, or within the top layer of sediments where biodegradation would have been greatest.

The hydrogen index has been used as an indicator of organic matter preservation (Demaison and Moore, 1980; Pratt, 1984; McArthur et al., 1992). Observations show that fresh marine plankton contain relatively high contents of lipids and other hydrogen-rich organic compounds. For example, organic matter accumulating in Quaternary sediments beneath the upwelling cell on the Peruvian continental shelf exhibits high HI of approximately 500 mg HC/g C_{org} (Emeis and Moore, 1990). Many authors have suggested that anoxic conditions developed within oxygen minimum zones are responsible for increased and well-preserved organic matter (e.g. Schlanger and Jenkyns, 1976; Demaison and Moore, 1980). More recent studies, however, have found no detectable difference between HI and TOC from modern surface sediments sampled from within and outside the oxygen minimum zone from the Gulf of California (Calvert et al., 1992a) and the eastern Arabian Sea (Calvert et al., 1995). These modern observations suggest that HI may not be affected by oxygen content of the bottom waters. Geochemical analysis conducted on refractory organic matter, however, does show that HI drops by 25–50% across the redox front within recent turbidite beds (McArthur et al., 1992). These results may imply that, over time, oxidized refractory organic matter may produce different geochemical signatures in anoxic and oxic sediments. Based on these observation, the consistently high values of HI for lithofacies B_1 compared to those from lithofacies B_{VAL} and B_2, may indicate a greater degree of labile organic matter preserved in lithofacies B_1.

Negative associations exist between Ox.I. and HI, HI* and TOC, and TOC against $\delta^{15}N_{tot}$ while a positive association exists between Ox.I. and $\delta^{15}N_{tot}$ from the Big Valley–Exshaw interval (Fig. 12). The lower HI, lighter $\delta^{13}C_{org}$, higher Ox.I. and heavier $\delta^{15}N_{tot}$ at low TOCs suggests a lower degree of organic matter preservation and generation at lower TOCs. Environmental conditions of lithofacies B_{BV} are interpreted to represent the lowest levels of primary production as indicated by the heavy $\delta^{15}N_{tot}$ values (Fig. 10). Bottom waters are considered to have been oxygenated based on the presence of bioturbation and the poor preservational quality (reflected by low HI (Fig. 3) and high Ox.I. (Figs. 3 and 11) and low quantity of organic matter (low TOC (Fig. 3)). The slightly lighter $\delta^{15}N$ isotope values of lithofacies B_2 (Fig. 10) may be interpreted as reflecting higher rates of primary production and organic matter supply to the sea floor. The quantity and quality of organic matter are also increased as demonstrated by higher HI and TOC (Fig. 3), and lower Ox.I. and $\delta^{13}C_{org}$ values (Figs. 3 and 10). Increased rates of recycling and grazing by heterotrophs, however, appear to have lowered the preservation potential and increased the refractory nature of this organic matter. Carbon supply to the sea floor is interpreted as having been highest, and organic matter recycling lowest, during deposition of lithofacies B_1 based on the light $\delta^{15}N_{tot}$ isotopes (Fig. 10) and the higher degree of preservation of labile organic matter as exhibited by the higher TOC and HI, but lower Ox.I. (Fig. 3).

Variations in productivity, export flux of labile organic matter and the eventual burial efficiency influenced organic matter geochemistry, affecting its quality and quantity. The relative supply of labile organic matter reaching the sediment–water interface can be demonstrated from the TOC vs. HI plot (Fig. 13(a)), which shows an asymptotic association. A similar asymptotic association between TOC and HI, derived from Kimmeridgian bulk mudrock and kerogen samples has been interpreted as indicating conditions of optimal organic matter preservation (Huc et al., 1992; Tyson, 1995). When plotting the hydrogen index derived from kerogen concentrates (HI*) against TOC (Fig. 13(b)) the relationship between HI* and TOC is no longer asymptotic, as mineral matrix effects (Peters, 1986) at low TOCs are taken into account. Bertrand and Lallier-Verges (1993); Bertrand et al. (1993) and Tribovillard et al. (1994) observed an asymptotic association between TOC and HI for Kimmeridgian clay samples, and interpreted HI as dominantly controlled by primary production levels, a higher ratio of labile/refractory organic matter reaching the sea floor and being buried during periods of high primary production. Similarly in this study the positive correlation between HI* and TOC is interpreted as indicating changes to the proportion of labile/refractory organic matter supplied to the sea floor at different rates of primary production (supported by the FTIR results).

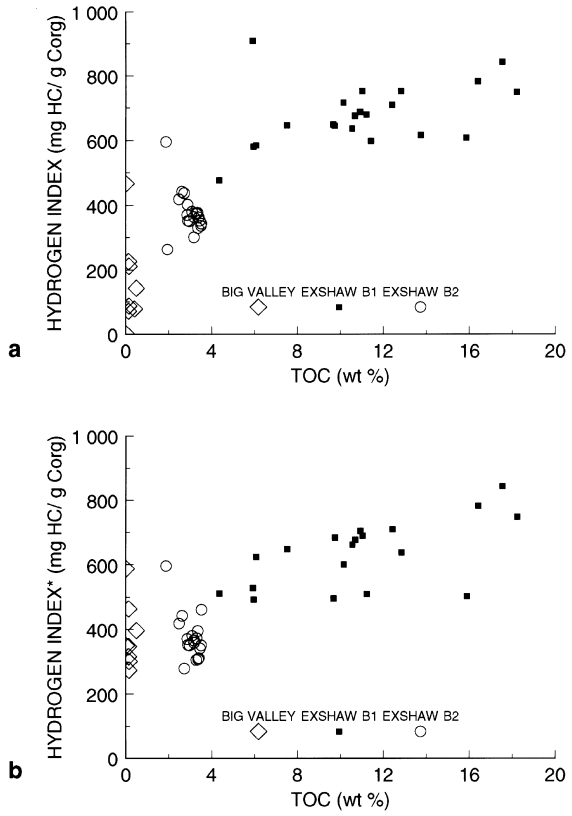

Fig. 13. Association between: (a) HI and TOC for bulk samples; and (b) HI* and TOC for kerogen concentrates from well 08-23-080-24W5. Note the asymptotic relationship in (a) and the linear relationship in (b).

Field observations have shown that eutrophic water columns are associated with better quality labile organic matter (Porter, 1976; Eppley and Peterson, 1979; Knauer et al., 1979; Pilskaln and Honjo, 1987).

6. Depositional model

The depositional model for the formation of contrasting mudrock sedimentary facies emphasizes that the fundamental control on organic matter quantity and quality was primary production (Fig. 14). A transgressive event during the Upper Devonian (Sandberg et al., 1988) resulted in flooding of the epicontinental sea with nutrient-rich water from the Panthalassa Ocean. Palaeoceanographic models predict the existence and position of an equatorial upwelling cell, which, extending across the entire Panthalassa Ocean, may have impinged on the North American continental shelf (Wright, 1994; Jewell, 1995; Whalen, 1995; Caplan et al., 1996) during the Upper Devonian transgression (Johnson et al., 1985). Intense oxygen utilization (of the upwelled water) resulting from degradation of settling organic matter, probably enhanced the development of benthic anoxia from Big Valley to Exshaw times. Development of eutrophic conditions promoted algal blooms and a rapid transfer of labile organic matter from the euphotic zone to the sea floor without much organic matter oxidation or recycling (indicated by high HI, TOC, low Ox.I., light $\delta^{15}N_{tot}$ and heavy $\delta^{13}C_{org}$), and the presence of phosphate and chert nodules, and radiolaria in lithofacies B_1.

In contrast, a eustatic sea-level fall at the D–C boundary (Sandberg et al., 1988) is recorded in the more distal regions of the epicontinental sea by deposition of lithofacies B_2 (Fig. 14(b)), where this lithofacies grades eastward into equivalent nearshore marine siltstones and sandstones of the Exshaw Formation in southeastern Alberta (Caplan, 1997). Sedimentological evidence in the form of breccias, volcanics and turbidites from the Earn Group in northern British Columbia and Yukon (Gordey et al., 1987), indicates that a topographical barrier may have been located far to the west of Alberta (Savoy and Mountjoy, 1995). This barrier may have restricted the influence of open marine currents and the eastward spread of upwelling currents from interacting with the epicontinental sea of the AUCP during the eustatic drop in sea-level, producing a shallow, broad basin. Mixing of the water column and promotion of regenerated production from remineralization of organic matter continued to support relatively low levels of primary production reflected by lower TOCs in lithofacies B_2. The organic carbon flux, however, was apparently still sufficient to create bottom water anoxia. Lower HI, TOC, higher Ox.I., heavy $\delta^{15}N_{tot}$ and light $\delta^{13}C_{org}$ of preserved organic matter in lithofacies B_2 can be explained by a drastic reduction in nutrient delivery to the euphotic zone, lower primary productivity, more intense grazing of the phytoplankton, enhanced recycling and more severe oxidation of organic matter in an oligotrophic sea.

7. Conclusions

Geochemical characteristics of Exshaw mudrocks of the Western Canada Sedimentary Basin imply that primary production was fundamental in controlling the level of organic richness and quality of this source rock. Black, laminated mudshales of lithofacies B_1 contain Type I/II organic matter, high TOC and HI, low Ox.I., heavy $\delta^{13}C_{org}$ and light $\delta^{15}N_{tot}$ values, whereas the laminated grey-green mudshales of lithofacies B_2 contain Type II/III kerogen, low TOC, HI and high Ox.I., light $\delta^{13}C_{org}$ and heavy $\delta^{15}N_{tot}$. Kerogen source variations, redox changes during diagenetic changes or

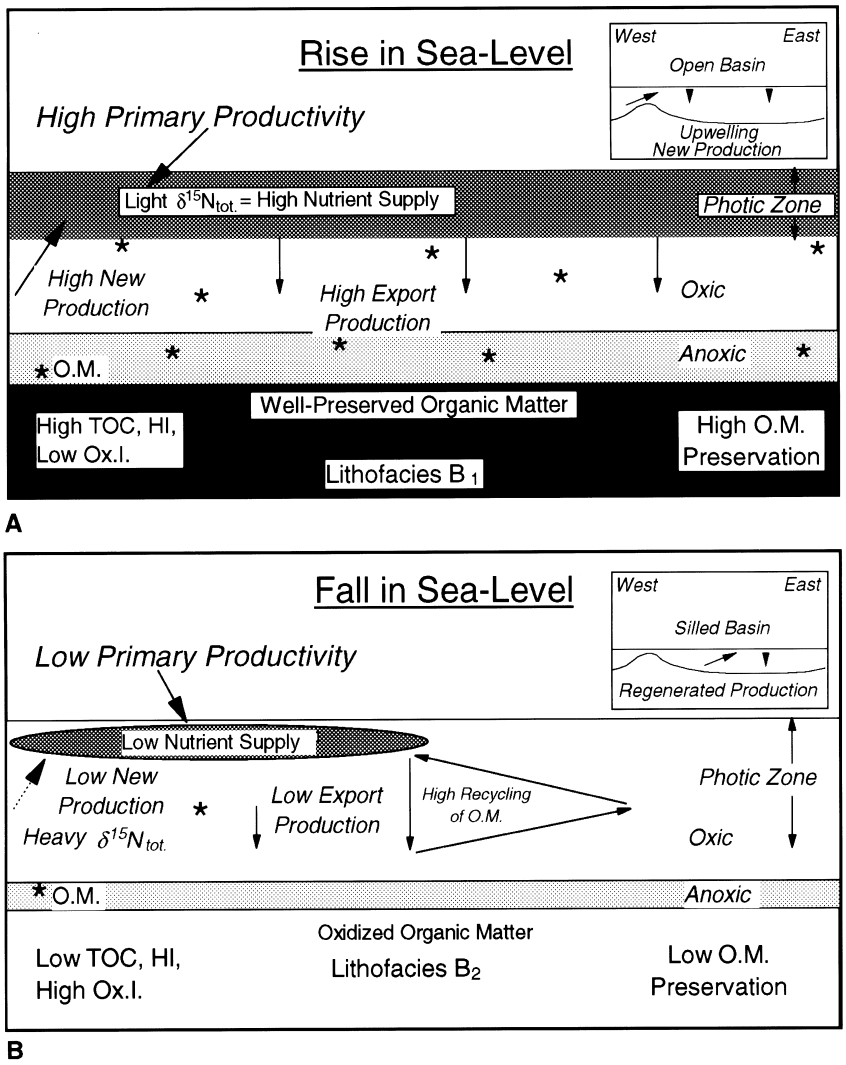

Fig. 14. Proposed depositional model for formation of contrasting organic matter geochemical characteristic of lithofacies B_1 and B_2. (a) Eastward migration of upwelling cell, during initial relative sea-level rise, promotes utilization of available dissolved oxygen and formation of an expanded OMZ. The OMZ is *not* responsible for the enhanced preservation of organic matter in lithofacies B_1. High TOC and HI of lithofacies B_1 reflects heightened primary production and higher supply of organic matter to benthic environment. (b) During the eustatic sea-level fall, upwelling efficiency is reduced. Organic matter is degraded and recycled in the water column many times before it is sedimented, thus its reduced inherent quality (lower TOC, HI and higher Ox.I.).

grain size changes are unsatisfactory in explaining these geochemical signatures. The pristine organic-rich deposits of lithofacies B_1 reflect eutrophic conditions in surface waters, higher primary production, as indicated by light $\delta^{15}N_{tot}$, and enhanced delivery of organic matter to the sea floor. In contrast, low rates of primary production (indicated by heavier $\delta^{15}N_{tot}$ values), low supply of organic matter to the sea floor and greater recycling of organic matter in the water column (reflected by low HI and high Ox.I.) resulted in lower quantity and quality of organic matter in lithofacies B_2 even though bottom waters appear to have remained anoxic.

Acknowledgements

We are grateful to Mobil Canada Ltd. for donating cores of Exshaw mudrocks. Maureen Soon (UBC) is thanked for generating XRD, XRF and CNS results, and Bente Nielsen (UBC) for determining the stable isotope results. Financial contributions were made by

the Geological Society of America, The Natural Science and Engineering Research Council (Canada), Amoco Canada Petroleum Company Ltd., Gulf Oil Canada, Shell Canada Ltd., UNOCAL Canada Ltd., Pan Canadian Petroleum Ltd. and Waskana Energy. Earlier versions of this manuscript benefitted from comments by Steve Calvert, Tom Pedersen, Paul Smith, Kurt Grimm and Maria Mastarlerz. We thank Lisa Pratt and Nicolas Tribovillard for their critical reviews of this manuscript.

Associate Editor—**S. George**

References

Allan, J., Creaney, S., 1991. Oil families of the Western Canada Basin. Bulletin of Canadian Petroleum Geology 39, 107–122.

Altabet, M.A, Francois, R., 1994a. The use of nitrogen isotopic ratio for reconstruction of past changes in surface ocean nutrient utilization. In: Zahn, R., Kaminski, M., Labeyrie, L.D., Pedersen, T.F. (Eds.), Carbon Cycling in the Glacial Ocean: Constraints on the Ocean's Role in Global Change. Springer, pp. 281–306.

Altabet, M.A., Francois, R., 1994b. Sedimentary nitrogen ratio as a recorder for surface ocean nitrate utilization. Global Geochemical Cycles 8, 103–116.

Barakat, A.O., Sadeghi, K.M., Yen, T.F., 1990. Fourier transform infrared analysis of partially oxidized kerogen concentrates. Fuel 69, 1055–1058.

Benalioulhaj, S., Trichet, J., 1990. Comparative study by infrared spectroscopy of the organic matter of phosphate-rich (Oulad Abdoun basin) and black shale (Timahdit basin) series (Morocco). Organic Geochemistry 16, 649–660.

Berner, R.A., 1994. Geocarb II: a revised model of atmospheric CO_2 over Phanerozoic time. American Journal of Science 294, 56–91.

Bertine, K.K., 1972. The deposition of molybdenum in anoxic waters. Marine Chemistry 1, 43–53.

Bertrand, P., Lallier-Verges, E., 1993. Past sedimentary organic matter accumulation and degradation controlled by productivity. Nature 364, 786–788.

Bertrand, P., Lallier-Verges, E., Boussafir, M., 1993. Enhancement of accumulation and anoxic degradation of organic matter controlled by cyclic productivity: a model. Organic Geochemistry 22, 511–520.

Betzer, P.R., Showers, W.J., Laws, E.A., Winn, C.D., DiTullio, Kroopnick, P.M., 1984. Primary productivity and particle fluxes on a transect of the equator at 153°W in the Pacific Ocean. Deep-Sea Research 31, 1–11.

Bustin, R.M., Cameron, A., Grieve, D, Wilks, K.R., 1985. Coal Petrography, its Principles, Methods and Applications. Geological Association of Canada, Short Course Notes, 2nd edition.

Calemma, V., Rausa, R., Margarit, R., Girardi, E., 1988. FTIR study of coal oxidation at low temperature. Fuel 67, 764–770.

Calvert, S.E., 1976. The mineralogy and geochemistry of near-shore sediments. In: Riley, J.P., Chester, R. (Eds.), Chemical Oceanography, Vol. 6. Academic Press, pp. 187–280.

Calvert, S.E., 1987. Oceanographic controls on the accumulation of organic matter in marine sediments. In: Brooks, J., Fleet, A.J. (Eds.), Marine Petroleum Source Rocks. Blackwell, pp. 137–151.

Calvert, S.E., 1990. Geochemistry and origin of the Holocene sapropel in the Black Sea. In: Ittekkot, V., Kempe, S., Michaelis, W., Spitzy, A. (Eds.), Facets of Modern Biogeochemistry. Springer, pp. 326–352.

Calvert, S.E., Pedersen, T.F., 1996. Sedimentary geochemistry of manganese: implications for the environment of formation of manganiferous black shales. Economic Geology 91, 36–47.

Calvert, S.E., Pedersen, T.F., 1993. Geochemistry of Recent oxic and anoxic sediments: implications for the geological record. Marine Geology 113, 67–88.

Calvert, S.E, Pedersen, T.F., 1992. Organic carbon accumulation and preservation in marine sediments: how important is anoxia? In: Whelan, J.K., Farrington, J.W. (Eds.), Organic Matter: Productivity, Accumulation, and Preservation in Recent and Ancient Sediments. Columbia Univ. Press, pp. 231–263.

Calvert, S.E., Bustin, R.M., Ingall, E.D., 1996. Influences of water column anoxia and sediment supply on the burial and preservation of organic carbon in marine shales. Geochimica et Cosmochimica Acta 60, 1577–1593.

Calvert, S.E., Bustin, R.M., Pedersen, T.F., 1992a. Lack of evidence for enhanced preservation of sedimentary organic matter in the oxygen minimum of the Gulf of California. Geology 20, 757–760.

Calvert, S.E., Nielsen, B., Fontugne, M.R., 1992b. Evidence from nitrogen isotope ratios for enhanced productivity during formation of eastern Mediterranean sapropels. Nature 359, 223–225.

Calvert, S.E., Pedersen, T.F., Naidu, P.D., von Stackelberg, U., 1995. On the organic carbon maximum on the continental slope of the eastern Arabian Sea. Journal of Marine Research 53, 269–296.

Caplan, M.L., Bustin, R.M., Grimm, K.A., 1996. Demise of a carbonate ramp by eutrophication. Geology 24, 715–718.

Caplan, M.L., 1997. Factors influencing the formation of organic-rich sedimentary facies: example from the Devonian–Carboniferous Exshaw Formation, Alberta, Canada. Unpublished Ph.D. thesis, University of British Columbia, p. 688.

Caputo, M.V., Crowell, J.C., 1985. Migration of glacial centres across Gondwana during Paleozoic Era. Geological Society of America Bulletin 96, 1020–1036.

Cowie, G.L., Hedges, J.I., 1992. The role of anoxia in organic matter preservation in coastal sediments: relative stabilities of the major biochemicals under oxic and anoxic depositional conditions. Organic Geochemistry 19, 229–234.

Demaison, G.J., Moore, G.T., 1980. Anoxic environments and oil source bed genesis. American Association of Petroleum Geologists Bulletin 64, 1179–1209.

Derenne, S., Largeau, C., Casadevall, E., Berkaloff, C., Rousseau, B., 1991. Chemical evidence of kerogen formation in source rocks and oil shales via selective preservation of thin resistant outer walls of microalgae: origin of

ultralaminae. Geochimica et Cosmochimica Acta 55, 1041–1050.

Dyrkacz, G., Bloomquist, C.A.A., Solomon, P.R., 1984. Fourier transform infrared study of high-purity maceral types. Fuel 63, 536–542.

Emeis, K.C, Moore, J.W., 1990. Organic carbon, reduced sulphur, and iron relationships in sediments of the Peru Margin, Sites 680 and 688. In: Suess, E., Von Huene, R. (Eds.), Proceedings ODP, Scientific Results, Vol. 112. National Science Foundation, pp. 441–453.

Eppley, R.W., Peterson, B.J., 1979. Particulate organic carbon flux and planktonic new production in the deep ocean. Nature 282, 677–680.

Espitalié, J., Madec, M., Tissot, B., Minnig, J.J, Leplat, P., 1977. Source rock characterization method for petroleum exploration. Proceedings of the 9th Annual Offshore Technology Conference, Houston, 1977, pp. 439–444.

Farrell, J.W., Pedersen, T.F., Calvert, S.E., Nielsen, B., 1995. Glacial–interglacial changes in nutrient utilization in the equatorial Pacific Ocean. Nature 377, 514–517.

Gordey, S.P., Abbott, J.G., Tempelman-Kluit, D.L., Gabrielse, H., 1987. "Antler" clastics in the Canadian Cordillera. Geology 15, 103–107.

Grimm, K.A., Lange, C.B., Gill, A.S., 1997. Self-sedimentation of phytoplankton blooms in the geological record. Sedimentary Geology 110, 151–161.

Hollander, D.J., Behar, F., Bertrand, P, McKenzie, J.A., 1990. Geochemical alteration of organic matter in eutrophic Lake Greifen: implications for the determination of organic facies and the origin of lacustrine source rocks. In: Huc, A.Y. (Ed.), Deposition of Organic Facies. A.A.P.G. Studies in Geology, 30, 181–193.

Huc, A.Y., Lallier-Verges, E., Bertrand, P., Carpentier, B, Hollander, D.J., 1992. Organic matter response to change of depositional environment in Kimmeridgian shales, Dorset, U.K. In: Whelan, J.K., Farrington, J.W. (Eds.), Organic Matter: Productivity, Accumulation, and Preservation in Recent and Ancient Sediments. Columbia University Press, pp. 469–486.

Ibach, L.E.J., 1982. Relationship between sedimentation rate and total organic carbon content in ancient marine sediments. American Association of Petroleum Geologists Bulletin 66, 170–188.

Jewell, P.W., 1995. Geologic consequences of global-encircling equatorial currents. Geology 23, 117–120.

Johnson, J.G., Klapper, G., Sandberg, C.A., 1985. Devonian eustatic fluctuations in Euramerica. Geological Society of America Bulletin 96, 567–587.

Jørgensen, B.B., 1982. Mineralization of organic matter in the sea bed: the role of sulphate reduction. Nature 296, 643–645.

Kister, J., Guiliano, M., Mille, G., Dou, H., 1988. Changes in the chemical structure of low rank coal after low temperature oxidation or demineralization by acid treatment. Fuel 67, 1076–1082.

Knauer, G.A., Martin, J.H., Bruland, K.W., 1979. Fluxes of particulate carbon, nitrogen and phosphorus in the upper water column of the northeast Pacific. Deep-Sea Research 26, 97–108.

Libes, S.M., 1992. An Introduction to Marine Biogeochemistry. Wiley, 733 pp.

Lin, R., Ritz, G.P., 1993a. Studying individual macerals using i.r. microspectroscopy and implications on oil vs. gas/condensate proneness and "low rank" generation. Organic Geochemistry 20, 695–706.

Lin, R., Ritz, G.P., 1993b. Reflectance FT-IR microspectroscopy of fossil algae contained in organic-rich shales. Applied Spectroscopy 47, 265–271.

Macqueen, R.W., Sandberg, C.A., 1970. Stratigraphy, age, and inter-regional correlations of the Exshaw Formation, Alberta Rocky Mountains. Bulletin of Canadian Petroleum Geology 18, 32–66.

Mastalerz, M., Bustin, R.M., Lamberson, M.N., 1993. Variation in chemistry of vitrinite and semifusinite as a function of associated inertinite content. International Journal of Coal Geology 22, 149–162.

Maynard, J.B., 1981. Carbon isotopes as indicators of dispersal patterns in Devonian–Mississippian Shales of the Appalachian Basin. Geology 9, 262–265.

McArthur, J.M., Tyson, R.V., Thomson, J., Mattey, D., 1992. Early diagenesis of marine organic matter: alteration of the carbon isotope composition. Marine Geology 105, 51–61.

Meijer Drees, N.C, Johnston, D.I., 1993. Geology of the Devonian–Carboniferous boundary beds in Alberta. In: Karvonen, R., Haan, J.D., Jang, K., Robinson, D., Smith, G., Webb, T., Wittenberg, J. (Eds.), Carboniferous to Jurassic Pangea-Core Workshop, C.S.P.G. and Glob. Sed. Geol. Prog., Calgary, pp. 188–205.

Montoya, J.P., 1994. Nitrogen isotope fractionation in the modern ocean: implications for the sedimentary record. In: Zahn, R., Kaminski, M., Labeyrie, L.D., Pedersen, T.F. (Eds.), Carbon Cycling in the Glacial Ocean: Constraints on the Ocean's Role in Global Change. Springer, pp. 259–280.

Müller, P.J., Suess, E., 1979. Productivity, sedimentation are and sedimentary organic matter in the oceans, 1. Organic carbon preservation. Deep-Sea Research 27A, 1347–1362.

Painter, P.C., Snyder, R.W., Starsinic, M., Coleman, M.M., Kuehn, D.W., Davis, A., 1981. Concerning the application of FTIR to the study of coal: a critical assessment of band assignments and the application of spectral analysis programs. Applied Spectroscopy 35, 475–485.

Pedersen, T.F., Calvert, S.E., 1990. Anoxia vs. productivity: what controls the formation of organic carbon-rich sediments and sedimentary rocks? American Association of Petroleum Geologists Bulletin 74, 454–466.

Pedersen, T.F., Shimmield, G.B., Price, N.B., 1992. Lack of enhanced preservation of organic matter in sediments under the oxygen minimum on the Oman margin. Geochimica et Cosmochimica Acta 56, 545–551.

Pelzer, E.E., 1966. Mineralogy, geochemistry and stratigraphy of the Besa River Shale, British Columbia. Bulletin of Canadian Petroleum Geology 14, 273–321.

Peters, K.E., 1986. Guidelines for evaluating petroleum sources rock using programmed pyrolysis. American Association of Petroleum Geologists Bulletin 70, 318–329.

Pilskaln, C.H., Honjo, S., 1987. The fecal pellet fraction of biogeochemical particle fluxes to the deep sea. Global Biogeochemical Cycles 1, 31–48.

Popp, B.N., Anderson, T.F., Sandberg, P.A., 1986. Brachiopods as indicators of original isotopic compositions

in some Paleozoic limestones. Geological Society of America Bulletin 97, 1262–1269.

Porter, K.G., 1976. Enhancement of algal growth and productivity by grazing zooplankton. Science 192, 1332–1334.

Pratt, L.M., 1984. Influence of paleoenvironmental factors on preservation of organic matter in Middle Cretaceous Greenhorn Formation, Pueblo, Colorado. American Association of Petroleum Geologists Bulletin 68, 1146–1159.

Rau, G.H., 1994. Variations in sedimentary organic $\delta^{13}C$ as a proxy for past changes in ocean and atmospheric CO_2 concentrations. In: Zahn, R., Kaminski, M., Labeyrie, L.D., Pedersen, T.F. (Eds.), Carbon Cycling in the Glacial Ocean: Constraints on the Ocean's Role in Global Change. Springer, pp. 307–322.

Richards, B.C., 1989. Upper Kaskaskia Sequence: Uppermost Devonian and Lower Carboniferous. In: Ricketts, B.D. (Ed.), Western Canada Sedimentary Basin, a Case History. C.S.P.G., pp. 165–201.

Richards, B.C, Higgins, A.C., 1988. Devonian–Carboniferous boundary beds of the Palliser and Exshaw Formations at Jura Creek, Rocky Mountains, southwestern Alberta. In: McMillan, N.J. (Ed.), Devonian of the World, Mem. 14, Vol. II. C.S.P.G., pp. 399–412.

Ripley, E.M., Shaffer, N.R., Gilstrap, M.S., 1990. Distribution and geochemical characteristics of metal enrichment in the New Albany Shale (Devonian–Mississippian), Indiana. Economic Geology 85, 1790–1807.

Rochdi, A., Landais, P., Burneau, A., 1991. Analysis of coal by transmission FTIR microspectroscopy: methodological aspect. Bulletin Société Géology de France 162, 155–162.

Rhoads, C.A., Senftle, J.T., Coleman, M.M., Davis, A., Painter, P.C., 1983. Further studies of coal oxidation. Fuel 62, 1387–1392.

Saller, A.H., Yaremko, K., 1994. Dolomitization and porosity development in the Middle and Upper Wabamun Group, southeast Peace River Arch, Alberta, Canada. American Association of Petroleum Geologists Bulletin 78, 1406–1430.

Sandberg, C.A., Poole, F.G., Johnson, J.G., 1988. Upper Devonian of Western United States. In: McMillan, N.J., Embrey, A.F., Glass, D.J. (Eds.), Devonian of the World, Proc. Can. Soc. Pet. Geol. Int. Symp., Devonian System I, pp. 183–220.

Savoy, L., 1992. Environmental record of Devonian–Mississippian carbonate and low-oxygen facies transitions, southernmost Canadian Rocky Mountains and northwesternmost Montana. Geological Society of America Bulletin 104, 1412–1432.

Savoy, L.E, Mountjoy, E.W., 1995. Cratonic-margin and Antler-age foreland basin strata (Middle Devonian to Lower Carboniferous) of the southern Canadian Rocky Mountains and adjacent Plains. In: Stratigraphic Evolution of Foreland Basins. S.E.P.M. Spec. Publ. 52, pp. 213–231.

Schlanger, S.O., Jenkyns, H.C., 1976. Cretaceous anoxic events: causes and consequences. Geologie en Mijnbouw 55, 179–184.

Suess, E., 1980. Particulate organic carbon flux in the oceans-surface productivity and oxygen utilization. Nature 288, 260–263.

Suess, E., Müller, P.J., 1980. Productivity, sedimentation rate and sedimentary organic matter in the oceans, II. Elemental fractionation. In: Daumas, R. (Ed.), Biogéochimie de la Matière Organique à l'Interface Eau–Sédiment Marine. Colloques Internationaux du C.N.R.S., Paris, No. 293, pp. 17–26.

Tissot, B.P, Welte, D.H., 1984. Petroleum Formation and Occurrence. Springer, 538 pp.

Tognotti, L., Petarca, L., D'Alessio, A., Benedetti, E., 1991. Low temperature air oxidation of coal and its pyridine extraction products. Fuel 70, 1059–1064.

Trask, P.H., 1939. Organic content of Recent marine sediments. In: Trask, P.H. (Ed.), Recent Marine Sediments. A.A.P.G., Tulsa, pp. 428–453.

Tribovillard, N.P., Desprairies, A., Lallier-Verges, E., Bertrand, P., Moureau, N., Ramdani, A., Ramanampisoa, L., 1994. Geochemical study of organic-matter-rich cycles from the Kimmeridge Clay Formation of Yorkshire (U.K.): productivity vs. anoxia. Palaeogeography Palaeoclimatology. Palaeoecology 108, 165–181.

Tribovillard, N.P., Gorin, G.E., Belin, S., Hopfgartner, G., Pichon, R., 1992. Organic-rich biolaminated facies from a Kimmeridgian lagoonal environment in the French Southern Jura mountains: a way of estimating accumulation rate variations. Palaeogeography Palaeoclimaology. Palaeoecology 99, 163–177.

Tyson, R.V., 1987. The genesis and palynofacies characteristics of marine petroleum source rocks. In: Brooks, J., Fleet, A.J. (Eds.), Marine Petroleum Source Rocks. Geol. Soc. Spec. Pub., Vol. 26, pp. 47–67.

Tyson, R., 1995. Sedimentary Organic Matter. Chapman and Hall, 615 pp.

Vine, J.D., Tourtelot, E.B., 1970. Geochemistry of black shale deposits: a summary report. Economic Geology 65, 253–272.

Wang, S.H., Griffiths, P.R., 1985. Resolution enhancement of diffuse reflectance i.r. spectra of coals by Fourier self-deconvolution, 1. C–H stretching and bending modes. Fuel 64, 229–236.

Wedepohl, K.H., 1978. Handbook of Geochemistry, Vols. I and II. Springer, Berlin.

Whalen, M.T., 1995. Barred basins: a model for eastern ocean basin carbonate platforms. Geology 23, 625–628.

Wignall, P.B., 1994. Black Shales. Clarendon, Oxford, 127 pp.

Wright, V.P., 1994. Early Carboniferous carbonate systems: an alternative to the Cenozoic paradigm. Sedimentary Geology 93, 1–5.